



HAWASSA UNIVERSITY
FACULTY OF ELECTRICAL ENGINEERING
DEPARTMENT OF ELECTRICAL AND COMPUTER ENGINEERING

PERFORMANCE COMPARISON OF PILOT-BASED CHANNEL
ESTIMATION METHOD IN OFDM SYSTEM OVER FADING CHANNEL

BY

HABTAMU ABEBE

ADVISOR:

DR. KINDE ANALY (Ph.D.)

Co- ADVISOR:

Mrs. LULSEGED TEFAYE (M.Sc.)

A THESIS

SUBMITTED TO THE DEPARTMENT OF ELECTRICAL AND COMPUTER
ENGINEERING IN PARTIAL FULFILLMENT OF THE REQUIREMENTS

FOR THE DEGREE OF MASTER OF SCIENCE
IN COMMUNICATION ENGINEERING AND NETWORKING

HAWASSA, ETHIOPIA

JUNE, 2019

ABSTRACT

Wireless channel is unknown and inclined to time dispersion, which causes inter symbol interference (ISI) and fading. OFDM is one of the most capable core technologies in the fourth generation of wireless communication systems. OFDM has the advantage over the conventional single-carrier modulation schemes when the channel is frequency-selective fading and widely used in current wireless networks. In this thesis work the performance of two pilot-based channel estimation algorithms; namely, least square (LS) and Minimum Mean Square Error (MMSE) with corresponding channel interpolation technique is investigated for digital communication systems. Channel estimation is a technique that can be used to design a channel in a particular surrounding based on known train symbols which is inserted in the input of transmitter end and tested at the receiver end.

This thesis performs , analysis of channel estimation algorithms based on bit error rate (BER) and signal to noise ratio (SNR) minimizing the error distance between the transmitted and received data. To estimate the channel coefficients; The MATLAB plot can perform for QAM, 16QAM, and 64QAM constellations. For different international telecommunication union (ITU) channel models Such as, the portable outdoor (PO), portable indoor (PI), Rural Area six path (RA6), Typical Urban six path (TU6), and Rayleigh channel models. Typical urban channel model has better at higher order modulation. From the MATLAB results, LS and MMSE algorithms are compared based on their pilot ratio and channel length. LS estimation has better at high SNR value compared to MMSE estimation.

Keywords: BER, Channel Estimation, LS, MMSE, OFDM, TU6

ACKNOWLEDGMENT

Next to GOD I would like to express my sincere gratitude to my advisor: Dr. Kinde Anlay (Ph.D.) for his continuous support, patience, motivation and immense knowledge. His guidance helped me in all the time of research and writing of this thesis.

I am also very grateful to my Co Advisor: Ins Lulseged Tesfaye (M.Sc.) supports me in many ways for successful accomplishment of this thesis.

Finally, I must also acknowledge communication staff member giving valuable motivation.

TABLE OF CONTENTS

ABSTRACT	ii
ACKNOWLEDGMENT	iii
LIST OF FIGURES	vii
LIST OF TABLE	viii
LIST OF ABBREVIATIONS	ix
LIST OF NOTATIONS	xii
Chapter One: Introduction	1
1.1. Background	1
1.2. Statement of the Problem	2
1.3. Objective	3
1.3.1. General Objective	3
1.3.2. Specific Objective	3
1.4. Literature Review	4
1.5. Scope and Limitation	8
1.6. Methodology	9
1.7. Contribution of Thesis	10
1.8. Thesis Organization	11
Chapter Two: OFDM and Fading Channel	12
2.1. Introduction	12
2.2. General Block Diagram of OFDM Transmitter and Receiver	12
2.3. Modulation and Demodulation	12
2.4. Transmitter Blocks of OFDM	13
2.4.1. Bit-Interleaved Coding and Modulation	14
2.4.2. FEC Channel Encoding	14
2.4.3. FFT-Frame Length of OFDM	15
2.5. OFDM Symbols Generation	15
2.5.1. Lines of Transmission in OFDM	16
2.5.2. Parameters in OFDM	16
2.5.3. Guard Interval	17
2.5.4. Train Symbol Pattern	18
2.5.5. Time Interleaving Factors	18
2.5.6. Superior of Code Rate, Block Length and Constellation	18

2.6. Block Diagram of OFDM Receiver	19
2.7. Multipath Propagation	20
2.7.1. Fading Channels.....	20
2.8. Small Scale Fading Channels.....	21
2.8.1. Small scale Fading Effects due to Multipath Time Delay Spread	21
2.8.2. Based on Doppler Effect	23
2.9. Channel Models for Orthogonal Frequency Division Multiplexing system	23
2.9.1. AWGN Channel Model	24
2.9.2. Rayleigh Fading Channel	25
2.9.3. Rician fading channel	26
2.10. Fixed Reception	27
Chapter Three: System Model.....	32
3.1. Channel Estimation	32
3.2. Block Type and Comb Type Train Symbol Arrangements	32
3.3. Mathematical Framework of Train Symbol-Based Channel Estimation	33
3.3.1. Least Square Channel Estimation Algorithm	34
3.3.2. Minimum Mean Square Channel Estimation Technique.....	35
3.3.3. LMS Based Channel Estimation.....	38
3.3.4. RLS Based Channel Estimation.....	39
3.4. Channel Interpolation Techniques	40
3.4.1. Piecewise Constant Interpolation and Linear Interpolation.....	40
3.4.2. Second-Order Interpolation.....	40
3.4.3. Cubic Spline Interpolation	41
3.4.4. DFT-Based Interpolation	41
3.4.5. MMSE Interpolation Technique.....	42
3.5. Blind Channel Estimation Techniques.....	42
3.6. Semi-Blind Channel Estimation Techniques	42
3.7. Selection Criteria of Channel Estimation Algorithms	43
Chapter Four: Result and Discussion	45
4.1: Channel estimation simulation diagram and channel model parameters	45
4.2.1. Performance comparison of different channel models	47
4.2.2. Channel estimation parameter for LS and MMSE.....	48
4.5. SNR VS BER performance comparison of LS and MMSE	50

4.5.2. Performance analysis of MMSE and LS channel estimation in different pilot size.....	51
4.6. Transmitted Original Image	53
4.7. Constellation Plot in Flat Fading channel.....	54
4.8. Constellation plot in frequency selective fading channel.....	55
4.8.1. Received image comparison for MMSE and LS Channel estimation Algorithm.....	57
4.8.2. Equalized image comparison for MMSE and LS Channel estimation Algorithm.....	57
Chapter Five: Conclusion and Future Work	59
5.1. Conclusion	59
5.2. Future Work.....	59
REFERENCE.....	61

LIST OF FIGURES

Figure 2.1: General Block Diagram of OFDM Transmitter and Receiver.....	12
Figure 2.2: Block diagram of an OFDM transmitter.....	13
Figure 2.3: Physical frame structure of OFDM	15
Figure 2.4: Block Diagram of OFDM Receiver	19
Figure 2.5: Multipath scattering of the signal	20
Figure 2.6: Channel model with fading coefficient and noise	24
Figure 2.7: AWGN channel model	24
Figure 3.1: Block and comb type train symbol arrangement	33
Figure 3.2: Minimum Mean Square Error channel Estimation.....	36
Figure 3.3: the block diagram of adaptive LMS algorithm is given below	38
Figure 4.1: Channel estimation simulation diagram	45
Figure 4.2: Different Channel Model for QAM.....	47
Figure 4.4: Different Channel model for 64QAM	47
Figure 4.5: BER vs SNR plot of LS and MMSE channel estimators for QPSK modulation.....	50
Figure 4.6: Performance comparison of LS and MMSE for different pilot sizes and CL	51
Figure 4.7: transmitted original image	53
Figure 4.8: received and estimated constellation plot.....	54
Figure 4.9: Constellation plot of MMSE equalizer at 15 dB SNR.....	55
Figure 4.10: Constellation plot of MMSE equalizer at 15 dB SNR.....	56
Figure 4.11: Received image comparison for MMSE and LS 15 dB	57
Figure 4.12: Equalized image for MMSE and LS at 15dB	57

LIST OF TABLE

Table 2.1: characterization of Rayleigh distribution.....	26
Table 2.2: Characterization of Rician Distribution.....	27
Table 2.3: wireless communication channel profile	31
Table 3.1: Computational complexity analysis.....	39
Table 3.2: Computational complexity analysis.....	44
Table 4.1: Channel model parameters.....	46
Table 4.2: channel estimation parameters.....	49
Table 4.3: Performance comparison of LS and MMSE.....	51
Table 4.4: channel estimation parameters.....	52

LIST OF ABBREVIATIONS

ADR	Astra Digital Radio
AWGN	Additive White Gaussian Noise
BH	Baseband Header
BCH	Bose-Chaudhuri-Hocquengham
BER	Bit Error Rate
BICM	Bit interleave Coded Modulation
CD3	Coded Decision Directed Demodulation
CE	Channel Estimation
CIR	Channel Impulse Response
CL	Channel Length
CMA	Constant Modulus Algorithm
COFDM	Coded Orthogonal Frequency Division Multiplexing
CR	Code Rate
CRC	Communications Research Center
DDA	Decision-Directed Algorithm
DFT	Discrete Fourier Transforms
DVB-C	Digital Video Broadcasting – Cable
DVB-T	First Generation Digital Terrestrial Television
DVB-T2	Second Generation Digital Terrestrial Television
FDM	Frequency Division Multiplexing
FEC	Forward Error Correction
FEF	Future Extension Frame
FFT	Fast Fourier Transformation
GA	Generic Algorithm
GI	Guard Interval
GIF	Guard-Interval Fraction
GCS	Generic Continuous Stream
GS	Generic Streams
GSM	Global System for Mobile Communications
HDTV	High Definition Television

HEM	High Efficiency Mode
HOS	Higher-Order Statistics
IFFT	Inverse Fast Fourier Transform
ISI	Inter symbol Interference
LAN	Local Area Network
LDPC	Low Density Parity Check
LMS	Least Mean Squares
LOS	Line Of Sight
LS	Least Square
MFN	Multi Frequency Network
MI	Modular Interface
MIMO	Multiple Input Multiple Output
MISO	Multiple Input Single Output
MLSE	Maximum-Likelihood Sequence Estimator
MPEG	Motion Picture Experts Group
MSE	Mean Square Error
NLOS	Non Line of Sight
NM	Normal Mode
NLMS	Normalized Least Mean Squares
OFDM	Orthogonal Frequency Division Multiplexing
PAPR	Peak to average Power Ratio
PDF	Power Delay Profile
PI	Pedestrian Indoor
PLP	Physical Layer Pipe
PO	Pedestrian Outdoor
QAM	Quadrature Amplitude Modulation
QPSK	Quadrature Phase Shift key
RA	Typical Rural Area
RF	Radio-Frequency
RLS	Recursive Least Square
RMS	Root Mean Square

RS	Reed-Solomon
SCR	Spectral Coherence Restoral
SDA	Steepest Descent Algorithm
SFN	Single Frequency Network
SISO	Single Input Single Output
SNR	Signal to Noise Ratio
SOS	Second Order Statistics STBC
TDT	Terrestrial Digital TV
TFS	Time Frequency Slicing
TI	Texas Instruments
TS	Transport Stream
TU	Typical Urban
TV	Television
UHF	Ultra-High Frequency
UP	User Packet
VBR	Variable Bit Rate
VHF	Very High Frequency
US	Uncorrelated Scattering
VSM	Vestigial Sideband Modulation
WAVE	Wireless Access in Vehicular Environment
WiMAX	Worldwide Interoperability for Microwave Access
WSS	Wide Sense Stationary
WSSUS	Wide Sense Stationary Uncorrelated Scattering
ZF	Zero Forcing

LIST OF NOTATIONS

$(.)^H$	Matrix Hermitian
$(.)^{-1}$	Matrix Inverse
$(.)^T$	Matrix (vector) Transposes
$(.)^*$	Complex Conjugate
$E \{.\}$	Mathematical Expectation
I_m	$M \times M$ Identity Matrix
RX	Receiver
TX	Transmitter
μ	Step Size

Chapter One: Introduction

1.1. Background

In the recent time, the rapid development of wireless communication technology has carried great convenience to people's lives and work. Digital communication technologies, especially mobile communication technology, presents unprecedented development. The objective of fourth generation mobile wireless communication system is to achieve ubiquitous, high-quality, high-speed mobile multimedia transmission [1]. To attain this goal, several new technologies are constantly being applied to mobile communication systems. OFDM is one of the most capable core technologies in the fourth generation of digital communication system [2, 3].

OFDM is one of the most widely used Modulation technique for high-bit-rate wireless communication. The Digital communication standards develop the prominence of OFDM shine brighter, especially when we consider the usage of smartphones as receiver. Wireless application corresponding High end Wireless local area network (HYPERLAN), Wireless Fidelity (Wi-Fi) and International Interoperability for Microwave Access (WiMAX) and also for Digital video broadcasting etc. Due to its high data rate transmission proficiency with high bandwidth efficiency and robustness to multipath delay. OFDM is being used as a standard scheme for the fourth generation of wireless communication systems [2]. Wireless communication device are in rely on multiple copies of the transmitted signals inward to the receiver through multiple paths [3, 4].

Channel estimation is used to obtain the channel state information to know the channel properties using blind channel estimation and train symbol-based channel estimation [4]. This information describes how a signal propagate from the transmitter to the receiver and represents the combined effect of fading, scattering and power decay with distance. The Channel State Information (CSI) makes it possible to adapt transmissions to current channel conditions, which is crucial for achieving reliable communication. In this thesis, the block train symbol based channel estimation technique is investigated. Channel estimation can be performed by either inserting train symbol tones into all of the subcarriers of orthogonal frequency division multiplexing symbols with a specific period or inserting train symbol tones into each orthogonal frequency division multiplexing symbols [3, 4]. The block type train symbol channel estimation is developed under the assumption of slow and fast fading channel.

1.2. Statement of the Problem

The main challenges in modern wireless communication systems are signal fading, ISI and low quality. Wireless communication introduced random and time varying channel. Due to multipath propagation and mobility of the channel and the receiver, many copies of transmitted signal attain at the receiver antenna at different instant of time with different attenuation and delay characteristics. So, these delayed signal components are separated by more ISI and symbol duration. Therefore, as a result of these distortions, wireless fading channels show dramatically poorer BER performance. The effect of the channel on the transmitted signal should be estimated correctly before equalization is made. The various techniques are compared using metrics such as computational complexity and performance for various channel variations in time and frequency domains. In choosing the proper channel estimation technique. The compared techniques, pilot assisted channel estimation is the most common techniques used in wireless communication for OFDM system.

To mitigate this challenging problem, wireless communication system designers employ digital channel estimation techniques that can minimize those undesired and destructive ISI effects and to improve low quality. Comparisons were focusing on optimal pilot ratio and channel lengths and limited to lower-order modulation for different fading channel with OFDM systems. However, investigating the performance of pilot-based channel estimation techniques for different pilot ratio and channel length in OFDM. The need for further study to understand the performance of different fading channel propagation effects in digital communication at higher order modulation schemes that include 16QAM and 64QAM is the motivation of this thesis.

1.3. Objective

1.3.1. General Objective

The main objective of this thesis is analysis of channel estimation algorithm in OFDM based on train symbol method using LS and MMSE algorithms for wireless communication over fading channel.

1.3.2. Specific Objective

- ✚ To analyze different channel model propagation performance for wireless network.
- ✚ To investigate and performance evaluation of the LS and MMSE channel estimation algorithms based on BER and SNR value.
- ✚ To analyze and compare the train symbol ratio and channel length effect for channel estimation techniques.
- ✚ To analyze the frequency selective and flat fading methods that can be used to mitigate the problem of ISI and multipath propagation to evaluate the received and equalized random data or image.

1.4. Literature Review

Here we cite a few references of work done related to channel estimation in wireless communication networks [5]. Evaluates the performance of channel estimation of LS and LMMSE. Performance analyze different channel models Using QAM, 16QAM and 64QAM as modulation schemes. It demonstrates performance of LS and LMMSE for wireless network channel estimators. Simulation results show that, LMMSE's performance for the same channel depends on pilot ratio and channel length and modulation scheme. However, this work is limited to pilot based channel estimation for slow fading channel.

In [6], the authors investigated the performance analysis of channel estimation using train symbol method. The time spread among first and neighboring signal in a multipath channel is called as multi path delay spread, which is seen by the receiver. This paper comprises of the performance analysis of train symbol procedure methods which are block type and comb type. At low and high SNR behavior of LS and MMSE are evaluated over AWGN channel for BPSK modulation et al relay on AWGN and Modulation scheme BPSK .The gap of this paper depends on those two channel models for AWGN and Rayleigh channel models. We analysis the channel model typical urban area and typical rural area channel models and increasing the modulation order to analysis the performance for wireless communication systems.

In [7], the authors investigated the correctness of channel estimation in OFDM system. CSI is required for signal detection at receiver side. The detection of signal affects the performance of system. Et al present, for lots of consistent communication it is important to enhance the channel estimation. Due to its high data rate capacity and robust to propagation environments fading and removing the ISI. In OFDM system, train symbol is inserted among subcarrier in transmitter side with equal spaced distance by using sampling theory and for channel estimation LS and MMSE technique is chosen. In OFDM frequency selective channels used which have appropriate performance due to these motives it is widely chosen in the field of study. Adding a LMS repetitive algorithmic rule to system, improves the channel estimation performance. Simulation results established the acceptable BER performance of repetitive channel estimation algorithm that is closed to the best channel. The low complexity projected receiver as well as LMS algorithmic rule is higher potency than typical methods and MMSE and it can be add low quantity of SNR. In adding to this work we investigates the channel models for wireless communication for consideration of indoor and outdoor for portable channel model effect.

In [8], the authors investigated estimation of channel in OFDM wireless channel using LS and MMSE technique, et al paper addresses two things in this work the first part of et al paper can be a comprehensive description of the system and a second part they describe the most applicable simulation, laboratory and T2 field trial results. The TS format is going to be used, these options should be selected, because in general no drawbacks are present. Sometimes padding could be needed to adjust the input stream packets to the BB Frames. In review of the literatures it is clear that various research mechanism has already been done on train symbol-based channel estimation techniques. However, in this paper has done on joint channel estimation and channel equalization do not clearly put channel estimation explicitly.

In [9], the authors investigated OFDM is a multi-carrier modulation scheme. Synchronization is the major problems of the OFDM system. The power consumption is considering through a noisy channel when an image frame is transmitted in the OFDM system. To support the work, many structures is tested such as minimizing the complexity with FFT/IFFTm. The size of bandwidth channel play the main role and how its effect on the transmission and how it's related to the FFT size (N_{fft}). The modulation type is also tested to see which one is the best for image transmitted. These types are phase shift keying and quadrature amplitude modulation. In addition, signal to noise ratio is one of the performances in OFDM system and consider one of the factors which wireless communication depends on related with bit error rate. Another problem of the OFDM system is PARR, therefore, the effect of N_{fft} on the PAPR has been tested with simulation results in which AWGN and Rayleigh channel models had been used in the simulation. The result is also a periodic variance of the coding error rates for several OFDM blocks. BER Vs SNR whereas apply no channel estimation and by spread on LS and MMSE as result obviously specified that LS methodology can be crack over higher signal to noise magnitude of intimate associate. in this work gap the analysis when the SNR value increase and channel length change the estimation value much difference so, not clearly put the result difference.

In [11], the authors investigated multiple signals are transmitted from different antennas at the transmitter using the same frequency and separated space. Various channel estimation techniques are employed in order to judge the physical effects of the medium present. In this paper, et al analyze and implement various estimation techniques for MIMO Systems such as LS and MMSE those techniques are therefore matched to successfully estimate the channel in MIMO System. The results confirm that SNR required to support different values of bit error rate varies depending on

different low correlation between the transmitting and the receiving antennas. In addition, it is explained that when the number of transmitter and receiver antennas increases, the performance of TBCE schemes significantly improves. The Same behavior is also observed for MIMO system. The Presentation of both MMSE and LS estimation are the similar for all types of modulation for different propagation environments for small value of SNR but in our work not only increasing the SNR value by increasing channel length and pilot ratio we have seen significant difference. The more we increase the SNR value also the more performance gap goes on increasing.

In [12], the authors investigated predominantly, the global spectral efficiency (SE) of both systems is investigated the partial spectral overlap between DVB and LTE signals occurs. Our contribution lies in double. The interfering signal modification in each network is derived analytically according to the frequency overlap while taking into account the difference between the characteristics of LTE and DVB networks, specifically the OFDM subcarrier spacing and then the OFDM symbol duration and SE is consequential with constant and non-uniform power distribution between overlapped and non-overlapped subcarriers of the two networks. This derivation offers an analytical evaluation of the effect of the spectral overlap ratio variation and diverse power allocation scenarios and offers perceptive results on the teamwork between the two networks. The gap of this paper, focus on fixed channel model type in our work considering mobility like that of the typical urban area and typical rural area channel models are examined so, means that the channel mobility consideration taken.

In [13], the authors investigated the AACE is an estimator which is established on the averaging of the last N Scattered train symbol from the DVB-T2 model carried in the received OFDM symbols. Et al proposed method to any pilot based estimator. The noise declared by the channel is considered as Additive White Gaussian Noise with zero mean and thus an averaging procedure is secondhand to eliminate it. The estimator adaptively follows the differences of the amplitude envelope in the time domain and adapts the size of the buffer N , with respect to the coherence time. Based on the averaged estimated channel, the LS or the LMMSE equalizer is applied to the received signal in the frequency domain. Simulations visibly display that the performance of the. Based on that AACE-LS is predictable LS estimator and is near to the performance of the MMSE with no need of a prior knowledge of the statistics and the noise of the channel and thus if the channel is unknown to the receiver, the AACE is a better choice conventional LS estimator and is near to the performance of the MMSE channel estimator is mysterious to the receiver. The Doppler

Spread introduced by the channel is a factor indicating the typical fading rate of the channel in the time domain. In the rest of the paper the channel assumed as Rayleigh. In the Logarithmic Envelope autocorrelation of the received signal is considered and a simple communication of the estimated Doppler frequency is derived. On considering the envelope autocorrelation of the received signal is considered and a simple expression of the estimated signal. In this thesis gap channel estimation not consider the shifted phase and inter symbol interference to recover the original data.

1.5. Scope and Limitation

The scope of this thesis work is analysis of the performance non-blind channel equalizers such as, LMS, LS and MMSE equalizers are to mitigate the flat fading and frequency selectivity effect. The MATLAB result the performance analyses and recommendation are based on BER vs SNR parameter using QAM and QPSK modulation. For MATLAB result, a random integer input generated using MATLAB's built-in function can be used for the BER comparison where stored and image source signal can be used to test. The thesis work does not include the implementation and analysis of blind and semi-blind types of equalization techniques.

1.6. Methodology

There are a couple of phases used to achieve the desired objectives of this thesis as follows.

Literature review: The first phase encompasses the reviews and study of various related literatures and e-books which help to understand the necessary theoretical background for research work related to multipath propagation and channel estimation techniques (i.e., blind, non-blind and semi-blind) and different channel estimation algorithms such as LS, LMS, RLS, and MMSE and also interpolation technique.

System model: On the second phase, theoretical analysis is carried out. And a system model, showing the processes using channel estimation algorithms for LS and MMSE for DVB-T2 system, showing their block diagram and description of block. Particularly when the train symbol is inserted at the transmitted OFDM subcarriers by the transmitter. At the receiver, the signal is detected, dividing it by the same channel response. Numbers of errors are calculated by comparing the transmitted and the received data. Signal and Noise power are calculated which then help in calculating the signal to noise ratio for the system.

Simulation: Simulating the modeled system using MATLAB software, performance comparison of channel estimation algorithms. This is approximation communication system model show the functionality test can be carried out with Generate arbitrary binary sequence of 1's and 0's mapping the binary sequence, multiply the symbols with the channel and then add white Gaussian noise, At the receiver, divide the received symbols with the known channel, Perform robust decision de mapping and sum of the errors and finally Repeat for multiple values of SNR and plot the simulation.

Performance comparison: Include comparing the BER-SNR, performance, computational complexity for the selected equalization techniques.

Analysis and interpretation of the results: Finally, the results are interpreted and conclusion is based on the result obtained.

1.7. Contribution of Thesis

In this research, the performance of wireless network communication system with QAM, 16QAM and 64QAM modulations in 8K mode of OFDM has been evaluated for the signals transmitted over the PI, PO, TU6, RA6 and Rayleigh fading channels. Some channel estimation approaches are integrated into the OFDM system model and their performances are tested under some situations. Comparing the performances revealed that the LS channel estimation method resulted in an acceptable performance for QPSK techniques at 15dB but MMSE is not good enough at 15dB to transmit high quality frame image over wireless network at this situation for thesis work.

1.8. Thesis Organization

This thesis contains five chapters; the first chapter contain an introductory which mainly consist the background, goal and motivational aspects of the thesis. The second Chapter presents the fading channel features and principle of OFDM transmission for wireless communication channels considered for this piece of work. In chapter three deals with system model as well as further mathematical detail description and for selected channel estimation algorithm. The fourth chapter includes result and discussion. The last Chapter is the conclusion and recommendation part of the thesis which tries to discuss the important conclusions drawn based on the results obtained from the whole thesis work.

Chapter Two: OFDM and Fading Channel

2.1. Introduction

Present day, OFDM is found in very contemporary and worldwide multimedia broadcast system like Digital Video and Audio Broadcasting i.e. (DVB), (DAB) , it is further launch in many dissimilarity wireless application corresponding High end Wireless local area network (HYPERLAN), Wireless Fidelity (Wi-Fi) and International Interoperability for Microwave Access (WiMAX) etc. OFDM is one of the special case of multi carrier transmission [13, 14].

2.2. General Block Diagram of OFDM Transmitter and Receiver

In the real implementation of OFDM, the combination of Fast Fourier Transform (FFT) and Inverse Fast Fourier Transform (IFFT) has been used to correlate frequency domain [14]. The correlation is just like mapping input onto sinusoidal basis function [14, 15]. In general by sending data which is in frequency domain through OFDM transmitter, it is turn to the time domain by IFFT block [15].

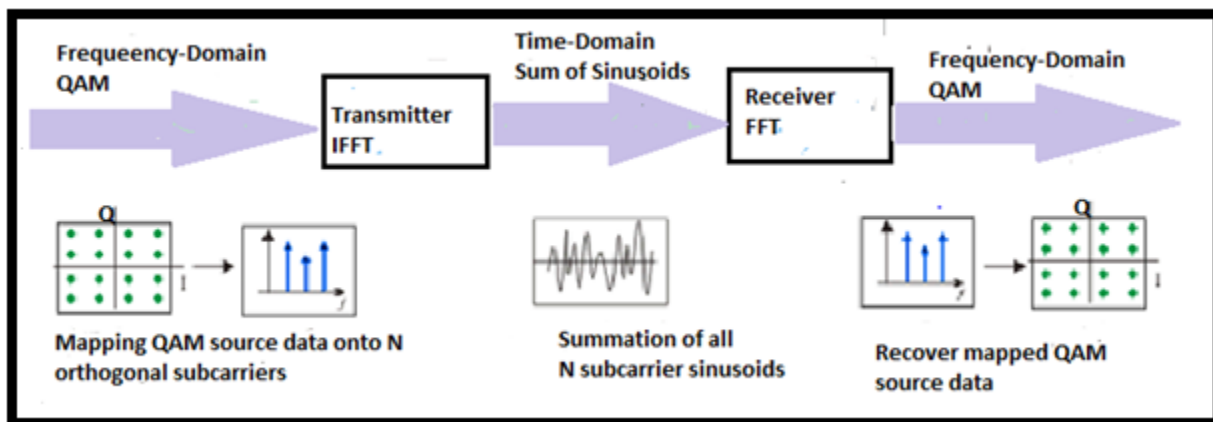


Figure 2.1: General Block Diagram of OFDM Transmitter and Receiver [15, 16]

2.3. Modulation and Demodulation

Major characteristics of the communication systems are which data lay on radio carriers. Systems are used to make this aim are called modulation. Modulation can be divided into analog and digital method; each of them has four dissimilar ways [14, 15]. In analog systems Amplitude Modulation (AM)), and QAM can be used. In the other side, for the digital systems, Phase Shift

Keying (PSK), Amplitude Shift Keying (ASK), and QAM can be used [17]. QAM is a combination of ASK and PSK which is widely used in OFDM systems [14].

2.4. Transmitter Blocks of OFDM

The generic block diagram of an OFDM transmitter is represented in Figure 2.2 below. As it can be seen, it is divided into four main parts; input processing, but not shown in the figure 3.2 input processing includes input data and encoder part, bit interleaved coded modulation (BICM), frame builder and OFDM generation [22,23]. The system inputs may be one or more High efficiency transport streams and or one or more generic streams. The input Pre-Processor, which is not part of the FFT system. It include a service splitter or de-multiplexer for FFT for separating the services into the FFT system inputs, which are one or more logical data streams [23, 24]. To explain in detail about the OFDM systems figure 2.2 below describe as follow [24].

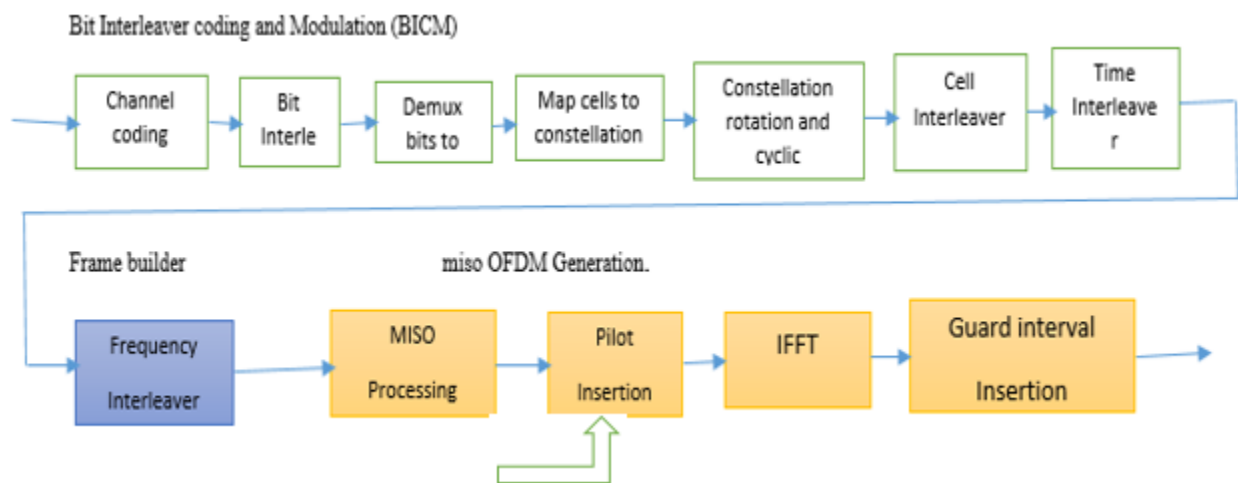


Figure 2.2: Block diagram of an OFDM transmitter [24, 25]

Input Processing: the OFDM standard, allows the following input formats transport Stream (TS). Stream with constant packet length, as in OFDM. Generic Encapsulated Stream (GSE) [25]. Constant or variable Length packets, where the format is known by the modulator. This format is intended to broadcast IP content without using TS-MPE (Multi-Protocol Encapsulation) [26]. Generic Continuous Stream (GCS). Variable length packets. Modulator does not know the actual length. Generic Fixed-length Packetized Stream (GFPS) [25, 26]. The input interface

subsystem shall map the input into internal logical-bit format. The first received bit is indicated as the Most Significant Bit (MSB). Input interfacing is applied separately for each single PLP [26]. CRC-8 encoding: CRC-8 is applied for error detection at UP level (Standard Mode and packetized streams only). When relevant, the UPL-8 bits of the UP (after sync-byte removal, when applicable) shall be processed by the systematic 8-bit CRC-8 encoder. The computed CRC-8 shall be appended after the user packet [26, 27].

Baseband Header (BBHEADER) Insertion: A digital data receiver practices baseband (BB) frames at both a base band (BB) block level and a terminal block level. At the BB block, the Digital receiver synchronizes BB frames from synchronization information inserted in the BB frame headers [27]. The BB block configures the error indicator based on whether an error is detected in the BB frame. Stream adaptation: Stream adaptation module takes a baseband header checked by a data field and sort by baseband frame. It include of three sub-modules: scheduler, Padding insertion and BB scrambling. Since our focus is on mode is skip the scheduling part [27, 28]. Padding insertion: When the baseband frame has insufficient data to fill it up or has the requirement to have an integer number of user packets, then padding is used to append zero bits after the data field to fill the frame [28]. BB scrambling: The main purpose of baseband scrambler is to ensure that the complete baseband frame is randomized and synchronization between the randomization sequence and the baseband frame [27, 28].

2.4.1. Bit-Interleaved Coding and Modulation

BICM module takes a baseband frame as input and produces an output for the next frame mapper. To carry out this task, the BICM shall perform outer coding (BCH), Inner Coding (LDPC), bit Interleaver and Demux for mapping bits to QAM constellation cells [28, 29].

2.4.2. FEC Channel Encoding

The purpose of the channel encoder is to introduce redundancy in the information sequence that can be used in the receiver to improve the effects of noise and interference, therefore improving the transmission reliability. LDPC is inner code which works well only for randomly distributed bit errors used to avoid regular patterns of errors and bursts of errors [28, 29]. BCH is outer code is included as an insurance against unwanted error floors at high C/N ratio [29].

2.4.3. FFT-Frame Length of OFDM

The T2-frame length is significant to boost the bit rate and the interleaving depth. The T2-frame length, or frame duration, depends on the FFT size, guard interval, and number of OFDM data symbols. It's a configurable parameter that is limited to a maximum value of 250 milliseconds [30]. To identify how the FFT-frame length disturbs the capacity and interleaving depth we have to look at the anatomy of the OFDM signal. The central building block of an OFDM system is called a Super Frame and be made up of number of FFT-frames, where each FFT-frame in turn consists of a number of OFDM-symbols. The P1 symbol is then followed by at least one P2 symbol that is used for signaling and data transmission [30, 31].

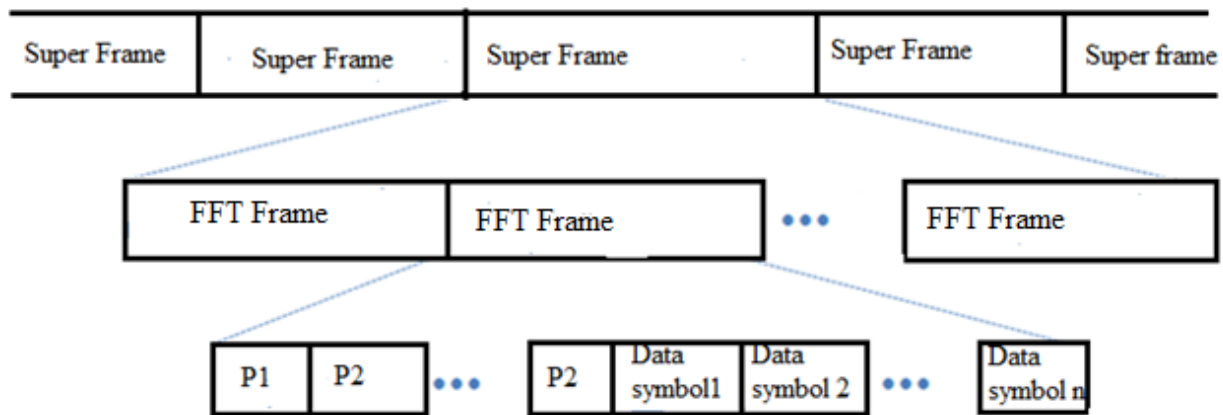


Figure 2.3: Physical frame structure of OFDM [31]

One can simply trust that a longer T2-frame length is result in an increase of whole bit rate due to the fact of the overhead associated with the preamble symbols P1 and P2 [29, 30]. To achieve the highest possible bit rate the number of dummy cells therefore need to be minimized a consequence of increasing the number of data symbols is of course that the number of OFDM cells per transmitted frame also increase[30,31]. This is because the FDM cells are now separated into one additional time interleaving block while the frame duration is increased only marginally [31].

2.5. OFDM Symbols Generation

OFDM Generation, The last block of the COFDM transmission chain is the generation of the OFDM symbols [32]. Six FFT sizes, 1K, 2K, 4K, 8K, 16K and 32K. Six channel bandwidths. 1MHz, 5 MHz, 6 MHz, 7 MHz, 8 MHz and 10 MHz Seven Guard interval fractions: 1/128, 1/32,

1/16, 19/256, 1/8, 19/128 and 1/4. For the 8K, 16K and 32K FFT sizes the extended carrier mode allows the use of large number of carriers per symbol which consequently improve the data capacity [31, 32]. Train Symbol Insertion Mechanism:-Train symbols are inserted in to encoded data cells. Which has known amplitude and phase that are used by the receiver to remove the ISI and compensate/equalize for channel impairments as the channel changes in frequency and in time [30]. The train symbols can be used for frame synchronization, frequency synchronization, time synchronization, channel estimation, transmission mode identification and can also be used to follow the phase noise [32]. Since OFDM is used as the modulation technique, so this sub-module performs IFFT in the transmitter to convert signal data from frequency domain to time domain [32, 33].

OFDM signals suffer from high Peak to Average Power Ratio (PAPR). OFDM provides two complementary techniques for reduction of PAPR ACE and Tone Reservation. One or both technique can be used simultaneously [33]. A channel estimation provides significant reduction in PAPR for lower order constellations (especially QPSK) while tone reservation provides greater benefit for higher order constellations [32]. A channel estimation increases the noise level that the receiver sees while transmission rate decreases but increases the throughput [32, 33].

2.5.1. Lines of Transmission in OFDM

Traditionally, all communication systems involve some core elements in order to operate and propagate the signal. Once all procedures that are necessary are completed, a mode of transmission is selected to feed the signal into the channel [32, 33]. The OFDM standard offered only the option of the SISO transmission of signals using a transmitting antenna on the provider's end and a receiving antenna on the receiver of the signal end [33]. OFDM standard steps forward to implement added modes of transmission. The system output that is typically transmitted over a radio frequency channel can support multiple output signals over multiple antennas. Thus, the new standard implements SISO, SIMO, MISO and MIMO transmission modes [33, 34].

2.5.2. Parameters in OFDM

There are a number of methods configuring an OFDM system. In this subsection we see the factors affecting the superior of each of the main parameters in turn [33]. The superior of the OFDM size depends on the application and expected channel Characteristics, so FFT gives the content

distributors a wide range of possible parameters to adapt to the desired behavior and expected channel suppositions [34].

2.5.3. Guard Interval

OFDM offers a wide range of possible guard intervals in order to support a range of transmission and broadcasting needs. We should distinguish between guard-interval duration TG; and guard interval fraction GIF= TG/ TU [47]. Assuming the channel extent for a particular transmission scenario is known, it is then a simple matter to choose a TG that suffices to match or exceed it [34, 35]. Note that this choice also require consideration of the FFT size. The greatest capacity is given by minimizing the GIF, which thus implies maximizing TU [33]. However, there are other constraints on the choice of FFT, concerning the degree of Doppler effects to be expected in the scenario of interest. These may set a limit to the FFT size (and thus TU) that can be chosen [35].

Transmitted OFDM signal waveform generated with CP is expressed as [33, 34]:

$$S(t) = \frac{1}{\sqrt{T_s}} \sum_{l' \in Z} \sum_{k'=0}^{N-1} X_{l'}[l'] e^{j2\pi \frac{k'}{T_s} t} \times \Pi\left(\frac{t-l'T+T_G}{T}\right) \quad (2.1)$$

Wireless communication networks are OFDM-based systems but with different physical characteristics and different parameters such as different subcarrier spacing and sampling frequency [34]. Let as define S (t) the transmitted signal T_s, T_G, N Transport streams (Ts) of OFDM symbol, the cyclic prefix (CP) durations and the number of OFDM subcarriers systems respectively.

Received Signal: In the wireless communication network, the signal received by Rx can be written as: [35]:

$$r(t) = \frac{1}{\sqrt{T_s}} \sum_{l' \in Z} \sum_{k'=0}^{N-1} \sum_{n'=1}^{L'} X_{k'}[l'] h_{n'} e^{j2\pi \frac{k'}{T_s} (t-\tau_{n'})} \times \Pi\left(\frac{t-\tau_{n'}-l'T+T_G}{T}\right) \quad (2.2)$$

Where r (t) received, $[l']$ the ODFM complex symbol of the $l' - th$ OFDM data block over the $k' - th$ OFDM subcarrier $h_{n'}$ is the Tx-Rx complex Gaussian distributed channel coefficient and its frequency response on the $k' - th$ subcarrier is given [50-51]

$$H_{k'} = \sum_{n'=1}^{L'} h_{n'} e^{-j2\pi \frac{k'}{T_s} \tau_{n'}} \quad (2.3)$$

The discrete signal is the projection of the received analog one on its waveform basis functions, i.e., OFDM waveform. Hence, the received signal at Rx on the $p' - th$ OFDM subcarrier and over the $m' - th$ OFDM data symbol is given by [33, 34]:

$$\tilde{X}_{p'}[m'] = \int_R r(t) \phi_{p',m'}(t) dt = \quad (2.4)$$

Where $\phi_{p',m'}^{(D)}(t)$ is the reception filter defined by?

$$\phi_{p',m'}(t) = \frac{1}{\sqrt{T_s^{(D)}}} e^{-j2\pi \frac{p'}{T_s} t \Pi(\frac{t-m'T}{T_s})} \quad (2.5)$$

Transmitter and Receiver are perfectly synchronized, the received OFDM signal can be written as [33, 34]:

$$[m'] = X_{p'}[m'] H_{p'}[m'] \quad (2.6)$$

2.5.4. Train Symbol Pattern

Superior of scattered train symbol pattern depends on guard interval and FFT size [33, 34]. There are exchange between the bandwidth efficiency and channel estimation accuracy regards the number of train symbols. The number of train symbols are reduce the bandwidth efficiency and channel estimation accuracy, it is very important that pilot pattern should be chosen carefully in OFDM system [35, 36]. The operator should choose a pilot pattern considering the expected channel for the type of usage that it is desired to support, and being aware of the trade-off between capacity and performance[35, 36].

2.5.5. Time Interleaving Factors

The sets of number of FFT blocks per interleaving frame depends on two factors. Increasing the number of FFT blocks for a given frame duration reduces the interleaving time, so reducing the time diversity and therefore the system's resistance to impulsive interference and fast time-varying channels [35, 36]. On the other hand, increasing the number of FFT blocks increases the maximum data rate for a PLP, since the maximum number of cells in a FFT block is fixed [36, 37].

2.5.6. Superior of Code Rate, Block Length and Constellation

The performance of LDPC codes is significantly better than convolutional codes used in OFDM system [37]. Consequently, the SNR requirement for a given LDPC code-rate is lower than for a convolutional code with the same code rate. Conversely, at a given SNR, a higher code rate can be used and therefore a higher data rate achieved [37, 38]. However, they can be used for low-bit-

rate applications requiring shorter latency. Alternatively, if long blocks are used for low-data-rate services, a user could choose either multi-frame interleaving (giving greater time diversity) or frame skipping (giving potential for power-saving); both options would entail a greater latency [38].

2.6. Block Diagram of OFDM Receiver

The main part of this thesis work i.e. channel estimation can be explain in the next chapter. The receiver comprises the above blocks in Figure 2.2 Most simply implement the reverse of the corresponding transmitter module [38, 39]. Three reverse of transmitter blocks are perform before channel estimation. The first block is P1 extraction used to removes and discards the P1 preambles. This module also removes and discards any FEF parts. The considerations for the use of the FFT algorithm in a receiver are essentially the same as those for the use of the IFFT in the modulator. We need to convert the time domain signal to frequency domain at the receiver [39].

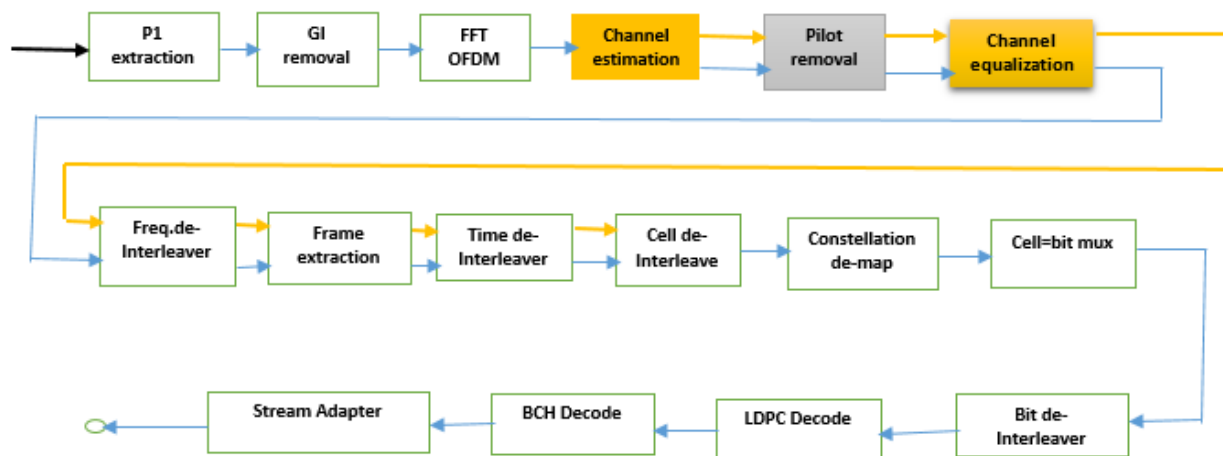


Figure 2.4: Block Diagram of OFDM Receiver [39, 40]

Frame extraction also reverse of frame builder; the receiver currently only processes one PLP, so this module only extracts the cells of this one PLP to feed to subsequent modules. The compensation of the channel effect is done at the receiver adjacent by applying synchronization, channel estimation and channel equalization [39, 40]. The main focus of our thesis work is implementation of channel estimation technique train assisted [40]. The detail of channel estimation techniques and algorithms for OFDM can be given in the next chapter

2.7. Multipath Propagation

The main features of wireless mobile channel are multipath propagation. The signal transmitting via the mobile channel from transmit antenna to mobile station antenna are not from a single path, but a number of different paths of many reflected waves [40, 41]. Because the path of electromagnetic wave, distance of transmission, emission coefficient of the launch point are different [40].

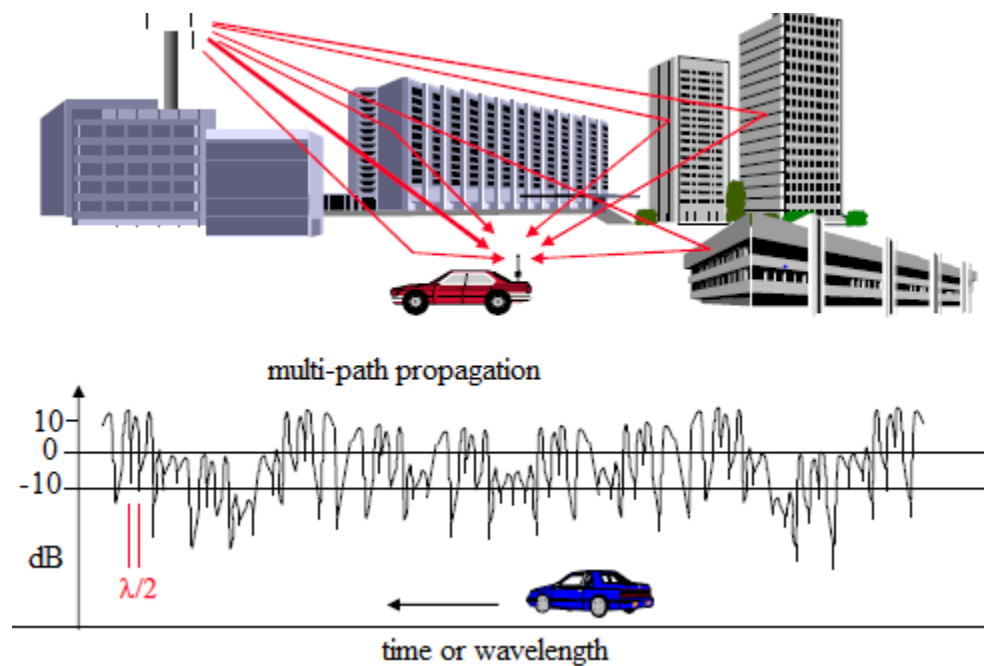


Figure 2.5: Multipath scattering of the signal [41, 42]

2.7.1. Fading Channels

When signal transmitted through the mobile wireless channel, signal fading features are determined by the transmitted signal and channel appearances [41]. Time dispersion and frequency selective fading are caused by multipath time delay spread, and frequency dispersion and time selective fading are caused by Doppler frequency spread [41, 42]. According to the frequency selectivity of channel, the channel can be divided into flat fading channels and frequency selective fading channel [42].

2.7.1.1. Large-Scale Fading

Large-scale fading happens as the mobile moves through a large distance and generated by path loss of signal as a function of distance and shadowing by large objects such as buildings, intervening terrains, and vegetation [42, 43]. Shadowing is a slow fading process described by variation of median path loss between the transmitter and receiver in fixed locations. In other words, large-scale fading is characterized by average path loss and shadowing [43]. Large-scale fading propagation models are used at the physical layer to expect the mean signal strength for a random transmitter-receiver departure distance. The free-space propagation model and the lognormal one are two generic propagation models that are often used as a basis for specific models [43, 44].

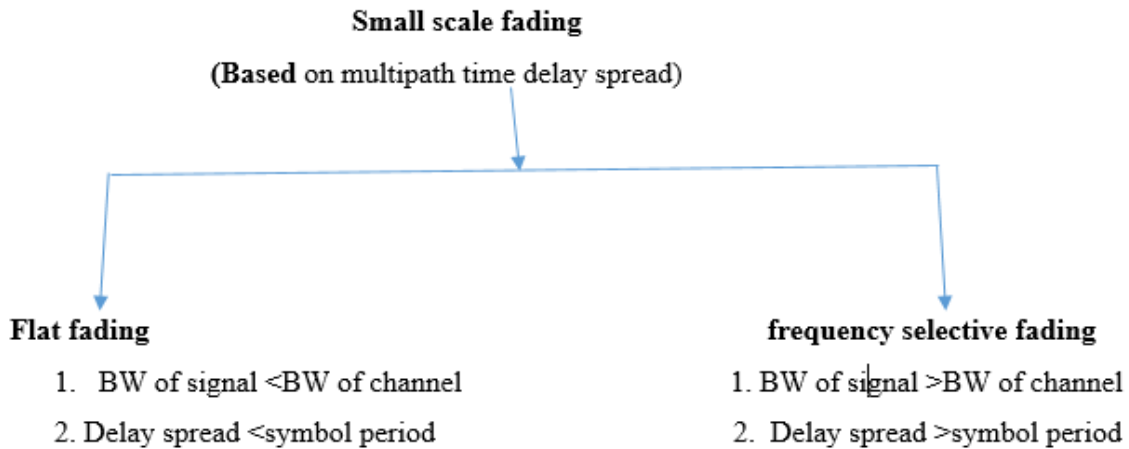
2.7.1.2. Lognormal Path Loss Propagation Model

A lognormal distributed random variable can be used to characterize the shadowing effects that occur with mean value determined by the transmitter and receiver separation distance [44]. A radio propagation model, also known as the Radio Wave Propagation Model or the Radio Frequency Propagation Model, are an empirical mathematical formulation for the characterization of radio wave propagation as a function of frequency, distance and other conditions [44].

2.8. Small Scale Fading Channels

The next classification of fading channel are Small-scale fading or basically fading which are used to describe the rapid fluctuations of the amplitude, phases, or multipath delays of a radio signal over a short period of time or portable distance, so that large-scale path loss properties ignored [44, 45]. Based on the relation between the signal parameters and the channel parameters (RMS delay spread and Doppler spread), we have different cases of fading [45]. Fading might have a time varying or frequency varying attenuating power on the Transmitted signal.

2.8.1. Small scale Fading Effects due to Multipath Time Delay Spread



2.8.1.1. Flat Fading

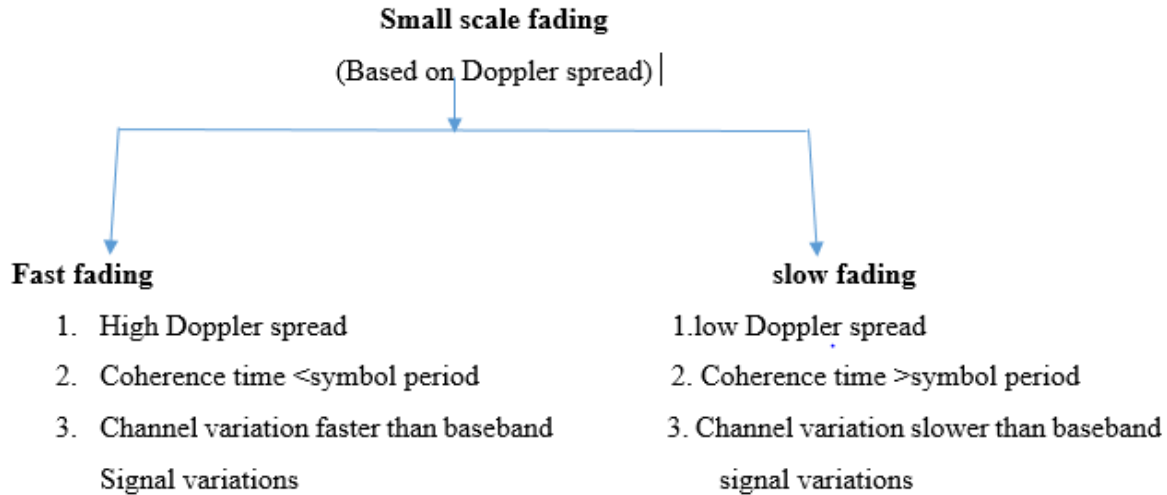
Small scale fading is distinctive as being flat or non-selective if the received multipath components of a symbol do not range elsewhere the symbol's time duration [44]. If the delay of the multipath components with respect to the key component are smaller than the symbol's time duration, a channel is said to be matter to flat fading [44,45]. In this fading channel Inter symbol interference (ISI) is absent; therefore, such a channel has a constant gain and a liner phase response over a bandwidth that is greater than the bandwidth of the transmitted signal [45]. In a flat-fading channel, the spectral characteristics of the transmitted signal are well-preserved at the receiver, and the channel does not cause any non-linear distortion due to time dispersion. However, the strength of the received signal generally changes slowly in time, due to the slow gain fluctuations caused by multipath. [45].

2.8.1.2. Frequency Selective Fading

Is a radio propagation anomaly caused by partial cancellation of a radio signal by itself the signal arrives at the receiver by two different paths, and at least one of the paths is changing (lengthening or shortening) [45]. This typically happens in the early evening or early morning as the various layers in the ionosphere move, separate, and combine. The two paths can both be sky wave or one be groundwave [44, 46]. As the carrier frequency of a signal is varied, the magnitude of the change in amplitude also vary, the coherence bandwidth measures the separation in frequency after which two signals are experience uncorrelated fading [46].

2.8.2. Based on Doppler Effect

The reason for the Doppler Effect are that when the source of the waves are moving towards the observer, each successive wave crest are emitted from a position closer to the observer than the previous wave. Therefore, each wave takes slightly less time to reach the observer than the previous wave [46, 47].



Fast fading: occurs when the coherence time of the channel is small comparative to the delay requirement of the application. In this case, the amplitude and phase change compulsory by the channel varies considerably over the period of use. In a fast-fading channel, the transmitter take advantage of the variations in the channel conditions using time diversity to help increase robustness of the communication to a temporary deep fade [47, 48].

Slow fading: Slow fading can be caused by events such as shadowing, where a large obstacle such as a mountain or large erection complicates the main signal path between the transmitter and the receiver. The received power change caused by shadowing is often modeled using a log-normal distribution with a standard deviation according to the log-distance path loss model [49].

2.9. Channel Models for Orthogonal Frequency Division Multiplexing system

When evaluating the complete performance of such communication systems, different channel models are used to model different transmission and reception scenarios [47, 48]. The frequency transfer function of a multipath fading channel are examined in terms of its effects on digital radio signals. The transfer function are expanded into a power series about the channel center frequency and the factor of related to the multipath model. Commonly used channel models are AWGN, Rayleigh, Rican, RA6, Portable indoor, portable outdoor and TU6 [48]. However, since each of

the models simulate a specific reception scenario, it are difficult to ascertain the realistic overall performance of the system [48]. As shown in the figure 2.6 below the received signal is attenuated by the fading coefficient and contaminated by noise.

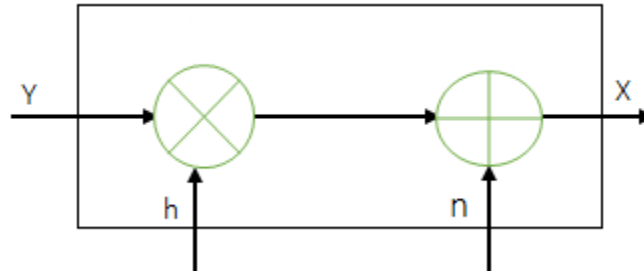


Figure 2.6: Channel model with fading coefficient and noise [47, 48]

The received signal of this channel model is given by:

$$y = h * x + n \tag{2.7}$$

Where Y is received signal, X is transmitted signal, **h** are a new fading coefficient and n are background noise or AWGN effect at the receiver that combines both the large-scale fading and flat fading [48]. The main job of channel estimation is to estimate the fading coefficients using appropriate channel models. There are many models that describe the phenomenon of small scale fading. Out of these models, AWGN, Rayleigh fading, Rician fading and COST 207 groups namely TU6 and RA6 [47,48].

2.9.1. AWGN Channel Model

The simplest radio environment in which a wireless communications system or a local positioning system or proximity detector based on Time of-flight have to operate are the AWGN environment. AWGN are the commonly used to transmit signal while signals travel from the channel and simulate background noise of channel [48].

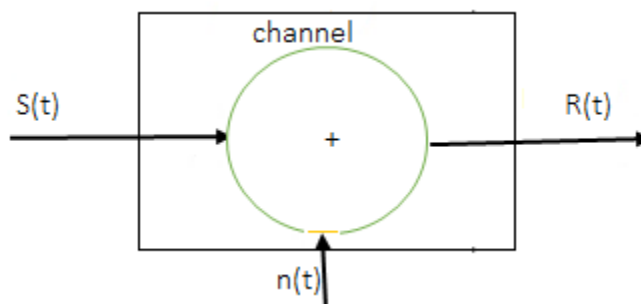


Figure 2.7: AWGN channel model [47-48]

The mathematical expression in received signal

$$R(t) = S(t) + n(t) \quad (2.8)$$

That passed through the AWGN channel where, the transmitted signal $s(t)$ and received $n(t)$ are background noise. An AWGN channel adds white Gaussian noise to the signal that passes through it. The basic communication channel model and used as a standard channel model. The transmitted signal gets disturbed by a simple additive white Gaussian noise process [48, 49].

2.9.2. Rayleigh Fading Channel

Rayleigh fading is considered as the most effective model for tropospheric and ionospheric signal propagation, as well as the effect of heavily built up urban environment on radio signals. Rayleigh fading is considered when there is no line of sight communication between the transmitter and receiver [47, 48]. If there is much scatter in the environment that scatter the radio signals before it arrives at the receiver, then in this case central limit theorem holds. Let $\{X_i, i = 1, 2, \dots, n\}$ be iid zero mean Gaussian random variables such that $X \sim N(0, \sigma^2) \forall i$ [48].

Then $X = \sqrt{\sum_{i=1}^n X_i^2}$ is defining as a generalized Rayleigh random variable when $n = 2$ in the equation, we get the Rayleigh distribution. Its PDF, CDF, MGF, raw moments, mean and variance are given in table 2.1 Rayleigh distribution is used to model small-scale fading in wireless communication channel when the channel is characterized by a large number of scatters and there is no dominant path or a line of sight connection. For instance, urban areas in mobile communication mostly have this kind of channel [47, 48].

Table 2.1: characterization of Rayleigh distribution [47, 48].

$$f_X(x) = \begin{cases} \frac{x}{\sigma^2} e^{-\frac{x^2}{2\sigma^2}} & x > 0 \\ 0 & x \leq 0 \end{cases} \quad (2.9)$$

$$F_X(x) = \begin{cases} 1 - e^{-\frac{x^2}{2\sigma^2}} & x > 0 \\ 0 & x \leq 0 \end{cases} \quad (2.10)$$

$$E[X^k] = (2\sigma^2)^{\frac{k}{2}} \Gamma\left(\frac{k}{2} + 1\right) \quad (2.11)$$

$$M_X(s) = M\left(1, \frac{1}{2}, \frac{1}{2}\sigma^2 s^2\right) + \sqrt{\frac{\pi}{2}} \sigma s e^{\frac{1}{2}\sigma^2 s^2} \quad (2.12)$$

$$E[X] = \sigma \left(\sqrt{\frac{\pi}{2}}\right) \quad (2.13)$$

$$\text{VAR}[X] = \left(\frac{4-\pi}{2}\right) \sigma^2 \quad (2.14)$$

2.9.3. Rician fading channel

Rician fading model is applicable most when in addition to scattering there is a strongly dominated signal seen at the receiver, usually caused by line of sight. During such random process, mean does not longer be zero [48]. In this case mean can vary around the power level of the dominant path. Let $\{X_i, i = 1, 2, \dots, n\}$ be independent Gaussian random variables with same variance but different mean such that $\sim N(0, \sigma^2), \forall i$ [47, 48]. Then $X = \sqrt{\sum_{i=1}^n X_i^2}$ is defined as a generalized Rician random variable. When $n = 2$ in the equation, we get the Rician distribution.

In what follows, we denote $a = \sqrt{\sum_{i=1}^n X_i^2}$. The Rician distribution descriptions are given in Table 2.2 Rice process is chosen as a suitable model of wireless channel when there is a dominant path or line of sight connection between the transmitter and receiver. Rural areas in mobile communication, for instance, usually possess this kind of channel. In the presence of a dominant or line-of-sight component, we get the sum of the scattered components and line of sight components at the receiver [48].

Table 2.2: Characterization of Rician Distribution [47, 48]

$$f_X(x) = \begin{cases} \frac{x}{\sigma^2} e^{-\frac{x^2-a^2}{2\sigma^2}} I_0\left(\frac{ax}{\sigma^2}\right) & x > 0 \\ 0 & x \leq 0 \end{cases} \quad (2.15)$$

$$F_X(x) = \begin{cases} 1 - Q_1\left(\frac{a}{\sigma}, \frac{x}{\sigma}\right) & x > 0 \\ 0 & x \leq 0 \end{cases} \quad (2.16)$$

$$E[X^k] = (2\sigma^2)^{\frac{k}{2}} e^{-\frac{a^2}{2\sigma^2}} \Gamma\left(1 + \frac{k}{2}\right) M\left(1 + \frac{k}{2}, 1, \frac{a^2}{2\sigma^2}\right) \quad (2.17)$$

$$E[X^2] = 2\sigma^2 + a^2 \quad (2.18)$$

$$E[X] = a \sqrt{\frac{\pi}{2}} M\left(-\frac{1}{2}, 1, \frac{a^2}{2\sigma^2}\right) \quad (2.19)$$

$$VAR[X] = E[X^2] - (E[X])^2 \quad (2.20)$$

According to central limit theorem the baseband equivalent of the sum is a complex Gaussian process. Furthermore due to the dominant path, the mean of the real part is different from zero. So the envelope of the impulse response is a Rice process [47, 48]. The situation is similar with a sinusoidal wave plus random noise which has been treated by Rice. In addition, the analysis based on experimental data in shows that Rician distribution is more accurate than Rayleigh distributions in modeling the signal statistics in rural or urban areas [50].

2.10. Fixed Reception

Receiver with a fixed rooftop antenna is called fixed reception which the antenna can be changed into two different usages. This outdoor antenna first can be set to receive the direct signal or in the worst case it can be set in order to receive the signal which has been reflected by different obtrusive objects such as buildings, hills or cars [51]. In the last stage, this antenna can reduce the echo of received signal and determine the main signal from distorted one [51, 52].

2.10.1. Portable Indoor (PI) and Portable Outdoor (PO)

Portable are specified to devices moving from one point to another. In this scenario, the reception does not moving very fast and the speed are assumed to be 3km/h. Wing-TV project has developed PI and PO channel models to define the slowly moving hand [52,53]

PI propagation environments: The power delay spectral density portable indoor for environments are given as [53]

$$S_{\tau}(\tau) = \begin{cases} C_{PI} e^{\frac{-\tau}{\mu s}}, & 0 \leq \tau < 5\mu s \\ C_{PI} \frac{1}{2} e^{\left(5 - \frac{\tau}{\mu s}\right)}, & 5\mu s \leq \tau < 10\mu s \\ 0, & else \end{cases} \quad (2.21)$$

Where, C_{PI} is a real valued constant coefficient given by:

$$C_{PI} = \frac{2}{3(1-e^{-5})} \quad (2.22)$$

The delay spread for PI propagation.

PO propagation environments [53]: the power delay spectral density for Portable Outdoor environments are given as:

$$S_{\tau}(\tau) = \begin{cases} C_{PO} e^{-3.5\tau/\mu s}, & 0 \leq \tau < 2\mu s \\ C_{PO} 0.1 e^{(15-\tau/\mu s)}, & 15\mu s \leq \tau < 10\mu s \\ 0, & else \end{cases} \quad (2.23)$$

Where, C_{PO} is a real valued constant coefficient given by:

$$C_{PO} = \frac{2}{3(1-e^{-5})} \quad (2.24)$$

The PO propagation, the power delay profile of each of the above propagation environments. The COST 207 models also specified four different Doppler spectra. These are; Jakes, GAUSE I, GAUSE II and RICE spectra [53, 54]. For any wireless communication system, non-line of sight components always present, as the signal are reflected from objects on the way from the transmitter to receiver.

2.11. COST 207 Channel Models

The COST 207 channel models for mobile radio is standardized to enable different communications designers to simulate their systems using a common set of channel models. Two propagation models are defined: (typical rural area –path6 (RA6), Typical urban area path6 (TU6) [54, 55]. Rural Area (RA) reception and typical urban (TU) reception. In addition to these models, a Rayleigh channel which is a theoretical channel with 6 paths reflected signals with no speed and fixed receptions using a rooftop outdoor antenna is employed [55].

2.11.1. RA6 and TU6 Propagation Environments

The mobile receptions bring high-speed propagation above 50 km/h. Mobile receptions are suffering from the factors such as AWGN, multipath propagation, narrowband interferers, and

impulse interferes [54, 55]. Following the channel variation, in time and frequency, in addition to noise handling needs strong synchronization [55].

The power delay spectral density for RA environments is given as:

$$S_{\tau}(\tau) = \begin{cases} C_{RA}e^{-9.2\tau/\mu s}, & 0 \leq \tau < 0.7\mu s \\ 0, & \text{else} \end{cases} \quad (2.25)$$

Where, C_{RA} is a real valued constant coefficient given by:

$$C_{RA} = \frac{9.2}{1-e^{-6.44}} \quad (2.26)$$

The delay spread for RA6.

Typical urban area propagation environments [55]:

Whereas, the power delay spectral density for TU environments is given as:

$$S_{\tau}(\tau) = \begin{cases} C_{TU}e^{-\tau/\mu s}, & 0 \leq \tau < 7\mu s \\ 0, & \text{else} \end{cases} \quad (2.27)$$

Where, C_{TU} is a real valued constant coefficient given by:

$$C_{TU} = \frac{1}{1-e^{-7}} \quad (2.28)$$

The TU6 propagation can be the focus of this thesis work. TU6 and RA6 propagation channel models reproduce the wireless communication propagation effects in an urban area and rural area respectively [54, 55]. The TU6 has been defined by COST 207 as a typical urban profile and are made of 6 propagations paths having wide dispersion in delay and relatively strong power [55]. In OFDM developments the TU6 propagation model is used for modeling mobility of the receiver [55].

The COST 207 models also specified four different Doppler spectra. These are; Jakes, GAUSE I, GAUSE II and RICE spectra [53, 54].

Jakes: The classical Jakes spectrum occurs only in the case of path delays less than 500ns, i.e., $\tau < 0.5\mu s$ and given by [53, 54];

$$S_{\mu\mu}(f) = \frac{1}{\pi f_d \sqrt{1-(f/f_d)^2}}, |f| \leq f_d \quad (2.29)$$

Where f_d represents the maximum Doppler frequency and the Doppler spread is $B_d = \frac{f_d}{\sqrt{2}}$

GAUS I: GAUS I is the sum of two Gaussian functions, occurs only in the case of path delays in the range of $500\mu s$ to $2\mu s$ i.e. $0.5\mu s \leq \tau < 2\mu s$ and is given by [52, 53]

$$S_{\mu\mu}(f) = G(A_1, -0.8f_d, 0.05f_d) + G(A_1/10, 0.4f_d, 0.1f_d) \quad (2.30)$$

Where $G(A_i f_i S_i)$ is defined as $A(A_1, f_1, S_1) = A_1 e^{-\frac{(f-f_1)^2}{2S_1^2}}$, (2.31)

The value of A_1 is by is given by $A_1 = \frac{50}{\sqrt{2\pi 3 f_d}}$, f_1 & S_1 are the values of the second and third terms of the Gaussian functions in Eq. (2.31) respectively. The Doppler spread for this case is given by $B_d = 0.45 f_d$ (2.32)

GAUSE II: GAUSE II is the sum of two Gaussian functions, occurs only in the case of path delays greater than $2\mu s$, i.e., $\tau \geq \mu s$ and is given:

$$S_{\mu\mu}(f) = G(A_2, 0.7 f_d, 0.1 f_d) + G\left(\frac{A_1}{10^{1.5}}, 0.4 f_d, 0.15 f_d\right) \quad (2.33)$$

Where $G(A_2 f_2 S_2)$ is given by $G(A_2 f_2 S_2) = A_2 e^{-\frac{(f-f_2)^2}{2S_2^2}}$ and the value of A_2 is given by

$$A_2 = \frac{10^{1.5}}{\sqrt{2\pi[\sqrt{(10+0.15)f_d}]}} \quad (2.34)$$

Ones again, f_2 & S_2 are the values of the second and third terms of the Gaussian functions in Eq. (2.30) respectively. The Gaussian functions in Eq. (2.34) respectively.

The Doppler spread for GAUSE II spectrum is $0.25 f_d$

RICE: Rice Doppler spectrum is obtained by combining the Jakes Doppler spectrum with and LOS component path. It is given by [53, 54].

$$S_{\mu\mu} = \frac{1}{\pi f_d \sqrt{1-(f/f_d)^2}} + 0.91 \sigma(f - 0.7 f_d), |f| \leq f_d \quad (2.35)$$

Table 2.3: wireless communication channel profile [51, 52]

Profile	Features	Path	Reception
Rayleigh	Rayleigh fading without Doppler shift	6 all is randomly realized with exponentials power delay profile with a dynamic range of 20dB	Fixed
PI	Direct path echoes with Doppler shift speed 3k/h	12 all pure Doppler	Portable
PO	Direct path echoes with Doppler shift speed 3km/h	12 all pure Doppler	portable
TU6	Rayleigh fading Urban area-speed 50 km/h	6 Rayleigh	Mobile
RA6	Rician fading Rural area- speed 100 km/h	1 Rician and 5 Rayleigh	Mobile

Chapter Three: System Model

3.1. Channel Estimation

In a wide sense, channel estimation defines any signal processing method used at the receiver to recover the fading channel, scattering dispersion and ISI problem is triggered by delay spread. Especially higher data-rate applications are more sensitive to delay spread signal and need high-performance channel estimation at the receiver or other ISI mitigation methods to be used at the transmitter side to make the signal less inclined to delay spread [56, 57]. The response of the channel at each subcarrier can be estimated from side to side at different interpolation methods which are based on known symbols are inserted at the transmitter part [57]. These symbols are called train symbols. The train symbols are inserted in to the OFDM subcarriers in different way. For this thesis we focus on the block type arrangements for slow channels to analysis frequency selective channel estimation using LS and MMSE algorithms. For different application wireless network communication system in the following sections [56, 57].

3.2. Block Type and Comb Type Train Symbol Arrangements

The block type train symbol insertion the time domain is technique applied. Figure 3.1 is the period of pilot tones which is applied on the time axis. In other words, estimation error has been reduced while each block is constant and it is the result of using all the subcarriers as pilots [57, 58]. The first one, block-type pilot channel estimation, is developed under the assumption of slow fading channel, and it is performed by inserting pilot tones into all subcarriers of OFDM symbols within a specific period. The second one, comb-type pilot channel estimation, is introduced to fulfill the need for equalizing when the channel changes even from one OFDM block to the subsequent one [58].

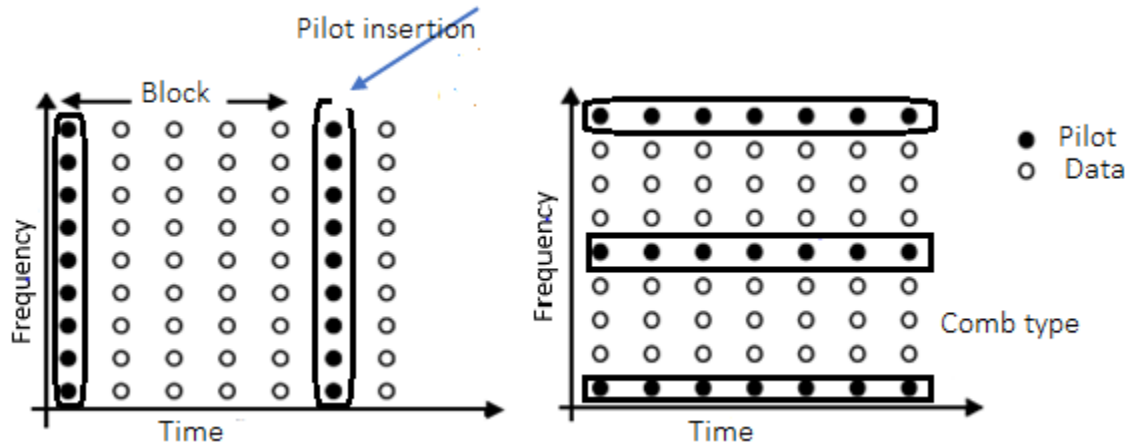


Figure 3.1: Block and comb type train symbol arrangement [58, 59]

The block-type train symbol arrangement are suitable for frequency-selective channels because train symbol tones are inserted into all subcarriers of train symbols with a period in time. For the fast fading channels, however, it might increase considerable overhead to track the channel variation by reducing the train symbol period [59]. The second comb type, the period of train symbol of tones in frequency, the train symbols must be placed as frequently as coherent bandwidths in order to track the frequency-selective channel characteristics. The coherence bandwidth is calculated by an inverse of maximum delay spread

3.3. Mathematical Framework of Train Symbol-Based Channel Estimation

For channel estimation, there have been a variety of algorithms with dissimilar optimization criteria and levels of numerical complexity [59]. The most common train symbol-based channel estimation algorithms are LMS, RLS, LS and MMSE. Iterative channel estimation algorithms LMS and RLS are suitable further down fast fading channels [58-59]. But these algorithms are commonly used for joint channel estimation and channel equalization our assumption are all subcarriers are orthogonal. The representation of the diagonal matrix of training symbols for N subcarriers are as follows.

$$X = \begin{pmatrix} X(0) & 0 & 0 \\ 0 & X(1) & 0 \\ 0 & 0 & X(N-1) \end{pmatrix} \quad (3.1)$$

Where $[k]$ denotes a pilot tone at the K^{th} subcarrier, with

$$\{[k]\} = 0 \text{ and } \{[k]\} = \sigma_x^2, k = 0, 1, 2, \dots, N-1. \quad (3.2)$$

By assumption all the subcarriers are orthogonal, X is a diagonal matrix. Representing the channel gain by $[k]$ for each subcarrier k , the train symbol of the received signal $[k]$ Can be represented in equation 3.2.

$$Y = HX + Z \quad (3.3)$$

Where H is the channel vector given as $H = [H(0), H(1), \dots, H(N - 1)]^T$ and Z is noise vector given as $Z = [Z(0), Z(1), \dots, Z(N - 1)]^T$ with $E\{Z(k)\} = 0$ and $var\{Z(k)\} = \sigma_z^2, k = 0, 1, \dots, N - 1$.

The main objective of thesis is estimating the channel coefficient \hat{H} using known pilot symbols. It can be discussed on the most common pilot based channel estimation algorithms, LS, MMSE in the following sections.

$$[Y] \triangleq \begin{bmatrix} Y[0] \\ \vdots \\ Y[N - 1] \end{bmatrix} = \begin{bmatrix} H[0] \\ \vdots \\ H[N - 1] \end{bmatrix} \begin{bmatrix} X[0] & \dots & 0 \\ \vdots & \ddots & \vdots \\ 0 & \dots & X[N - 1] \end{bmatrix} + \begin{bmatrix} Z[0] \\ \vdots \\ Z[N - 1] \end{bmatrix} \quad (3.5)$$

3.3.1. Least Square Channel Estimation Algorithm

The goal of the channel least square estimator is to minimize the square error distance between the received signal and the original signal. Denoting the channel estimate by \hat{H} the Least Square Channel estimation technique becomes the channel estimate by minimizing the following cost [60, 61].

$$J(\hat{H}) = \|Y - X\hat{H}\|^2 \quad (3.6)$$

$$(Y - X\hat{H})^H (Y - X\hat{H}) \quad (3.7)$$

$$= Y^H Y - Y^H X \hat{H} - \hat{H}^H X^H Y + \hat{H}^H X^H X \hat{H}$$

In order to minimize we set the derivative of the function with respect to \hat{H} zero, i.e.

$$\frac{\partial J(\hat{H})}{\partial \hat{H}} = -2(X^H Y)^* + 2(X^H X \hat{H})^* = 0 \quad (3.7)$$

Computing Equation 3.7 we get, $X^H X \hat{H} = X^H Y$ and from this we get the solution to the LS channel estimation as:

$$\hat{H}_{LS} = X^H X^{-1} Y = Y^{-1} Y \quad (3.8)$$

Denoting each component of the LS channel estimate \hat{H}_{LS} by $\hat{H}_{LS}[K]$, where $K=0, 1, \dots, N-1$ based on the assumption of orthogonality i.e. ICI free mode, the Least square channel estimate \hat{H}_{LS} can be written for each sub carrier as the following equation:

$$\hat{H}_{LS}[K] = \frac{Y[k]}{X[k]}, \text{ where } K=0, 1, 2 \dots N-1 \quad (3.9)$$

After having \hat{H}_{LS} the LS channel estimate, we can calculate the Mean Square Error (MSE) of the LS channel estimation technique by

$$MSE_{LS} = E \left\{ (H - \hat{H}_{LS})^H (H - \hat{H}_{LS}) \right\} \quad (3.10)$$

$$= E \{ (H - X^{-1}Y)^H (H - X^{-1}Y) \}$$

$$E \{ (X^{-1}Z)^H (X^{-1}Z) \} \quad (3.11)$$

$$= E \{ Z^H (XX^H)^{-1} Z \}$$

$$\frac{\sigma^2_Z}{\sigma^2_X} \quad (3.12)$$

As shown in Equation 3.8 the MSE of LS channel estimation is inversely proportional to Signal to Noise Ratio (SNR) $\frac{\sigma^2_Z}{\sigma^2_X}$ it implies that it is subject to noise enhancement, especially when the channel is in a deep null. Although LS technique has the above problem, as a result of mathematical simplicity it has been widely used for channel estimation [60].

3.3.2. Minimum Mean Square Channel Estimation Technique

Take the Least Square solution in the Equation 3.9 $\hat{H}_{LS} = X^{-1}Y \triangleq \tilde{H}$ and using a weight matrix W , define $\hat{H} \triangleq W\tilde{H}$ which corresponds to MMSE [60].

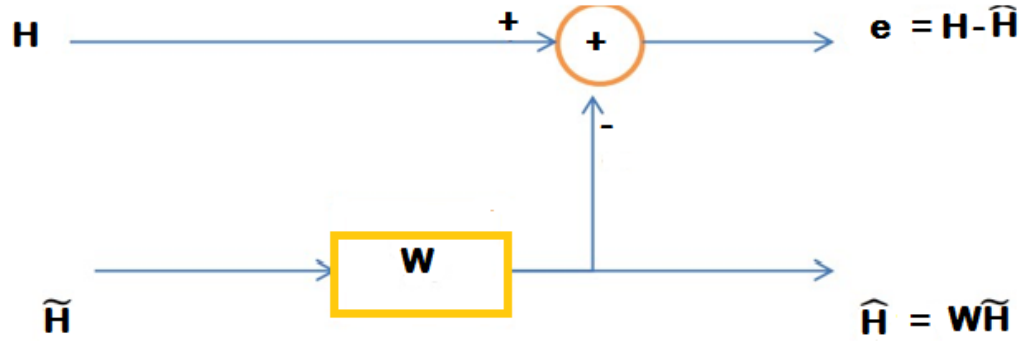


Figure 3.2: Minimum Mean Square Error channel Estimation [60, 61-62]

From the Figure 3.2 we can see that MSE of the channel estimate \hat{H} is given by

$$J(\hat{H}) = E\{\|e\|^2\} = E\{\|H - \hat{H}\|^2\} \quad (3.13)$$

From this the MMSE channel estimation process finds a better estimate in terms of W in such a way that the MSE in Equation 3.13 is minimized. The orthogonality principle states that the estimation error vector $e = H - \hat{H}$ is orthogonal to \tilde{H} such that

$$E\{e\tilde{H}^H\} = E\{(H - \hat{H})\tilde{H}^H\} \quad (3.14)$$

$$E\{(H - W\tilde{H})\tilde{H}^H\} \quad (3.15)$$

$$= E\{H\tilde{H}^H\} - WE\{\tilde{H}\tilde{H}^H\}$$

$$R_{H\tilde{H}} - WR_{\tilde{H}\tilde{H}} = 0 \quad (3.16)$$

Where $R_{H\tilde{H}}$ is the cross correlation matrix of $N \times N$ matrices H and \tilde{H} (i.e. $R_{H\tilde{H}} = E[H\tilde{H}^H]$), and \tilde{H} is the Least Square channel estimate given by

$$\tilde{H} = X^{-1}Y = H + X^{-1}Z \quad (3.17)$$

Solving Equation 3.10 for W results

$$W = R_{H\tilde{H}}R_{\tilde{H}\tilde{H}}^{-1} \quad (3.18)$$

Where $R_{\tilde{H}\tilde{H}}$ is the auto correlation matrix of \tilde{H} given by

$$R_{\tilde{H}\tilde{H}} = E\{\tilde{H}\tilde{H}^H\} \quad (3.19)$$

$$=E\{X^{-1}Y(X^{-1}Y)^H\}$$

$$E\{(H + X^{-1}Z)(H + X^{-1}Z)^H\} \quad (3.20)$$

$$=E\{HH^H + X^{-1}ZH^H + HZ^H(X^{-1})^H + X^{-1}ZZ^H(X^{-1})^H\}$$

$$=E\{HH^H\} + E\{X^{-1}ZZ^H(X^{-1})^H\}$$

$$E\{HH^H\} + \frac{\sigma_z^2}{\sigma_x^2} \mathbf{I} \quad (3.21)$$

And $R_{H\tilde{H}}$ is the cross-correlation matrix between the true channel vector and temporary channel estimate vector in the frequency domain. From the Equation 3.21, the MMSE channel estimate solved as:

$$\hat{H} = W\tilde{H} \quad (3.22)$$

$$=R_{H\tilde{H}}R_{\tilde{H}\tilde{H}}^{-1}\tilde{H}$$

$$R_{H\tilde{H}}(R_{HH} + \frac{\sigma_z^2}{\sigma_x^2} \mathbf{I})^{-1}H^{-1} \quad (3.23)$$

The elements of $R_{H\tilde{H}}$ and R_{HH} in the above equation 3.20

Where: $R_{HH} = E\{HH^T\}$ is the autocorrelation matrix of the

Channel, $\beta = \{ |X_k|^2 \} E \left\{ \left| \frac{1}{X_k} \right| \right\}^2$ is a constant related to the chosen QAM constellation diagram

(for 16-QAM, $\beta=17/9$), the SNR is expressed as $SNR = \frac{E\{|X_k|^2\}}{\delta_n^2}$ and δ_n^2 denotes the variance of noise $E\{|n_k|^2\}$ The Mean Squared Error in case of MMSE is given in 3.24

$$MSE_{MMSE} = (H - \hat{H}_{MMSE})^H \cdot (H - \hat{H}_{MMSE}) \quad (3.24)$$

$$E\{h_{k,1}\tilde{h}^*_{k',1'}\} = E\{h_{k,1}h^*_{k',1'}\} = r_f[k - k']r_t[1 - 1'] \quad (3.25)$$

Where K and 1 denote the subcarrier frequency index and OFDM symbol time index, in that order. In a practical system, the channel autocorrelation and SNR can be set to known factors at the receiver in advance. The channel autocorrelation calculation and SNR estimation affect the performance [61, 62]. Compared with the LS method, MMSE method this is improved but extra complex because this must estimate the inverse of the channel estimation matrix therefore more calculations. Additionally, MMSE algorithm requires knowledge of channel covariance and noise variance, which are assumed to be known as a priori knowledge. The LS algorithm does not need any knowledge about the channel autocorrelation [62].

3.3.3. LMS Based Channel Estimation

Reminder that the steepest-descent algorithm can be implemented only if the correlation matrix and the cross-correlation vector are known. Although this can be achieved by estimating through time averaging, this is a cumbersome procedure. In this way, the true gradient is replaced with a so-called random process or noise gradient [62]. Defines the so-called LMS adaptive filter. Remark that the filter coefficients (also called filter weights) are updated by adding a term to $W_k[n]$ is proportional to the current error output $e[k]$ and to the delayed filter input $X[k-n]$ [62, 63]

The LMS is a search algorithm in which an interpretation of the gradient vector computation is made probable by appropriately modifying the objective function. The LMS algorithm, as well as others related to it is widely used in various applications of adaptive filtering due to its computational simplicity [63].

The block diagram of adaptive LMS algorithm is given below.

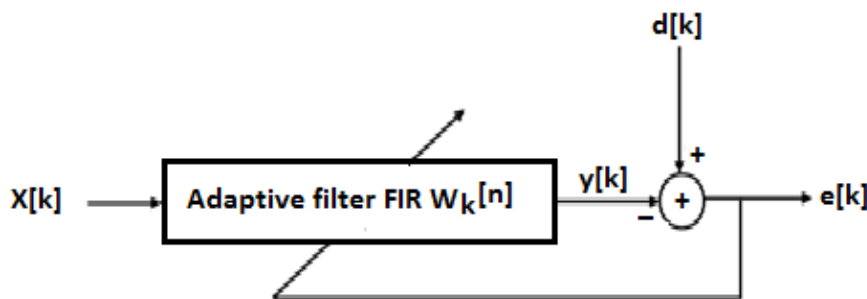


Figure 3.3: the block diagram of adaptive LMS algorithm is given below [62, 63].

For a real-time implementation in total $N+1$ memory cells are needed for the filter weights, N cells for past inputs $x[k-n]$, and about 4 cells for $e[k]$, $d[k]$, $x[k]$, μ , The block processing delay of the (N) LMS adaptive filter is typically one sample. The LS algorithm does not need any knowledge about the channel autocorrelation [63].

3.3.4. RLS Based Channel Estimation

The Recursive Least Squares (RLS) adaptive filter is an alternative to the LMS algorithm. It can be derived by minimizing the following deterministic cost function. The minimum of the cost function is found by setting the gradient to zero. Given that a matrix inverse is involved the required number of arithmetic operations rises with N^3 [63]. The idea behind the RLS adaptive filter is to compute the optimal weights W_{k+1} starting from W_k rather than computing from scratch.

Table 3.1: Computational complexity analysis [61, 64]

Algorithms	Advantages	Disadvantages	Comments
LMS	Easier to implement than RLS	Require straining Sequence.	Commonly used for joint channel estimation And Equal.
RLS	Always converges faster than LMS	Requires training sequence, computationally complex	Commonly used for joint channel estimation and Equalization.
LS	Very easy to implement	Doesn't correlate with noise	Can be used for explicit channel estimation
MMS E	Fast convergence than LS	Very high Complexity i.e. Requires matrix Inversion.	Can be used for explicit channel estimation

Since the objective of this thesis is for extracting the channel coefficients independently the simulation concentrates on LS and MMSE channel algorithms only.

3.4. Channel Interpolation Techniques

The channel estimation based on comb type train symbol insertion, an interpolation technique is necessary in order to estimate channel at data sub-carriers by using the channel information at train symbol sub-carriers [62,63].train symbol data symbols are inserted at a regularly Interval in actual block of data. According to the pilot allocation scheme the train symbols can be inserted in the time or frequency domain to estimate the channels for a particular time instant or subcarriers. However, the channels for data symbols are unknown to the receiver except the train symbol channel estimates [63]. The interpolation techniques are needed to estimate the channels between subcarriers or time slots.

3.4.1. Piecewise Constant Interpolation and Linear Interpolation

We call it piecewise constant interpolation (or nearest neighbor interpolation). It allocates same train symbol values to near data subcarriers [64]. The optimal number of train symbols for a given BER can be determined in advance for OFDM systems with numerical evaluation as in [61, 64]. The channel estimation at the data subcarrier is obtained by estimation of response of two end-to-end train symbol sub-channels. But the requirement is linearity of transmitted functions of adjacent sub-channels. The linear interpolation is shown as below:

$$\bar{H}(k)=\bar{H}(mN_f + l) = \left(\bar{H}_p(m + 1) - \bar{H}_p(m) \right) Nf + \bar{H}_p(m), m = 0,1 \dots N_p - 1 \quad (3.26)$$

In Equation 3.16 above, in the linear interpolation estimation only first two nearest data points are interpolated this train symbol interpolated data points used estimate the channel this very simple method [63].

3.4.2. Second-Order Interpolation

Second order interpolation is better than linear interpolation, where the channel estimation at the data subcarrier is calculated by used linear combination of three adjacent train symbols [63].

Theoretically, high order interpolation yields enhanced channel estimation because of using more train symbols. And the channel estimation can be close to the true channel response. But computation complexity is increased as increasing of order [63, 64]. The channel estimation of second order interpolation is given by:

$$\bar{H}(k)=\bar{H}(mN_f + l) = c_1\bar{H}_p(m - 1) + c_0\bar{H}_p(m) + c_{-1}\bar{H}_p(m1), m = 0,1, \dots \dots N_p - 1 \quad (3.27)$$

The coefficients are defined as

$$C_1=\frac{\alpha(\alpha-1)}{2} \quad (3.28)$$

Where $C_0=-(\alpha - 1)(\alpha + 1)1, \alpha = \frac{1}{N_f}$

$$= C_{-1}=\frac{\alpha(\alpha-1)}{2}$$

3.4.3. Cubic Spline Interpolation

The cubic spline interpolation method produces a smooth and continuous polynomial fitted to given data points [63, 64]. The fundamental idea behind spline cubic interpolation is based on draw smooth curves through a number of points [64], which is given by:

$$\bar{H}(k) = \bar{H}(mN_f + l) = a_1\bar{H}_p(m + 1) + a_0\bar{H}_p(m) + N_f a_1 \bar{H}'_p(m + 1) - N_f a_0 \bar{H}'_p(m), m = 0,1 \dots \dots N_p - 1 \quad (3.29)$$

Where $\bar{H}'(m)$ is the first derivative of $\bar{H}(m)$ and

$$\alpha_1 = \frac{3(N_f-l)^2}{N_f^2} - \frac{2(N_f-l)^2}{N_f^3} \quad (3.30)$$

$$\alpha_1 = \frac{3l^2}{N_f^2} - \frac{2l^2}{N_f^3}$$

Although cubic spline interpolation with higher order interpolation can be used for better interpolation accuracy, the performance improvement is not obviously proven [64].

3.4.4. DFT-Based Interpolation

The DFT-based interpolation technique is the output of the Fourier transform of the channel impulse response. The DFT-based interpolation effectively removes the effects of noise

outside the maximum channel delay spread or the length of multipath channel. The implementation of the DFT-based interpolation is also straightforward compared to the linear or second-order interpolation, but the length of multipath channel must be known to the receiver [64, 65]. DFT based interpolation technique individual requires FFT and IFFT computation as well as the length of multipath, so it is a very common approach used in channel estimation for OFDM systems [64].

3.4.5. MMSE Interpolation Technique

Compared to other interpolation techniques, MMSE interpolation can be the most real way to estimate the channels between train symbols with the aid of statistical information [64]. The channels such as, the channel correlation and SNR have been additional computation of the matrix inversion. However, it can be achieved an admirable performance as compared to linear, second-order and DFT-based interpolation [65].

3.5. Blind Channel Estimation Techniques

Blind channel estimation technique method is provide a route for every individual symbol of OFDM for channel estimation. In this algorithm complexity is the one of the maximized issue introduced and their required the additional train symbol to complete a recovered phase. To cope with this problem of complexity a modification is applied in maximum likelihood method described in [65].

In maximum likelihood method to indecision the phase indistinctness in the adjacent subcarriers different modulation schemes applied. Related to mutually the techniques, later you've high complexity, which can increase since the constellation order increase. How much, load capacity is reduced as the numbers of pilots are increased [65, 66]. As the train symbols are used for channel estimation, by associating pilot sequence at the receiver side can be find the channel state. The train symbols are transmitted with the payload symbol with time domain it cost and count as the overhead in transmission system [67].

3.6. Semi-Blind Channel Estimation Techniques

Semi-Blind system require less computational complexity than blind methods and rarer training symbols than training-based methods, making them attractive for practical implementation [67]. Semi-blind algorithms can recover the performance of blind

algorithms by exploiting the knowledge of both known symbols and possessions of the transmitted signals. The objective of semi-blind channel estimation algorithm is to get better performance than blind algorithms although requiring rarer known symbols than training based channel estimation algorithms [68].

3.7. Selection Criteria of Channel Estimation Algorithms

For one estimation technique, there may exist several adaptive algorithms that could be used to estimate the weight vector. The optimal of one algorithm over another is strongminded by several issues which include [67, 68]:

Rate of convergence: - This is defined as the number of iterations required for the algorithm, in response to stationary input, to converge to the optimum solution [67].

Computational complexity: - refers to the number of operations (multiplications, divisions, and additions/subtractions) required to update the filter from one time instant to the subsequent [67].

Numerical properties:-The numerical accuracy and stability of the algorithm refers to error minimization capability of the algorithm [67, 68].

Miss adjustment:-For an algorithm of interest, this parameter provides a quantitative measure of the amount by which the final value of the MSE [68].

Analysis summary

Table 3.2 shows the complexity analysis of all estimators: After analysis the complexity evaluation it can be established that LS estimator stretches the lowest complexity because it consists of only one multiplication and one inverse operation and the MMSE estimator gives the highest computational complexity [68].

Table 3.2: Computational complexity analysis [67, 68]

Estimation scheme	Number of operations needed	Complexity	Comments
LS estimator	$n(n + 1)$	Lowest	Simple matrix multiplication and inverse operation
MMSE estimator	$n^2(2n + 3)$	Very High	Large number of matrix multiplications
LMS	$2n + 1$	LOW	Doesn't require matrix inversion
RLS	$4n^2$	High	More complex than LMS but easier than MMSE

Chapter Four: Result and Discussion

4.1: Channel estimation simulation diagram and channel model parameters

In this chapter, MATLAB results and discussions are based on the obtained results. MATLAB-based plot is used to investigate the performances of different channel models with different modulation order and comparison of LS and MMSE channel estimation algorithms. In this thesis performance analysis of channel coefficients using LS and MMSE algorithms in frequency selective channels and adjust the shifted phases using LMS algorithm in flat fading channels. The simplified channel estimation simulation diagram of OFDM system for different application of wireless network communication systems. In Figure 4.1 below, the complete OFDM system model is very challenging. In the goal of this analysis with complex simulation model with reduced complexity. From the below simulation diagram figure 4.1 the entire system includes transmitter, channel and receiver diagram.

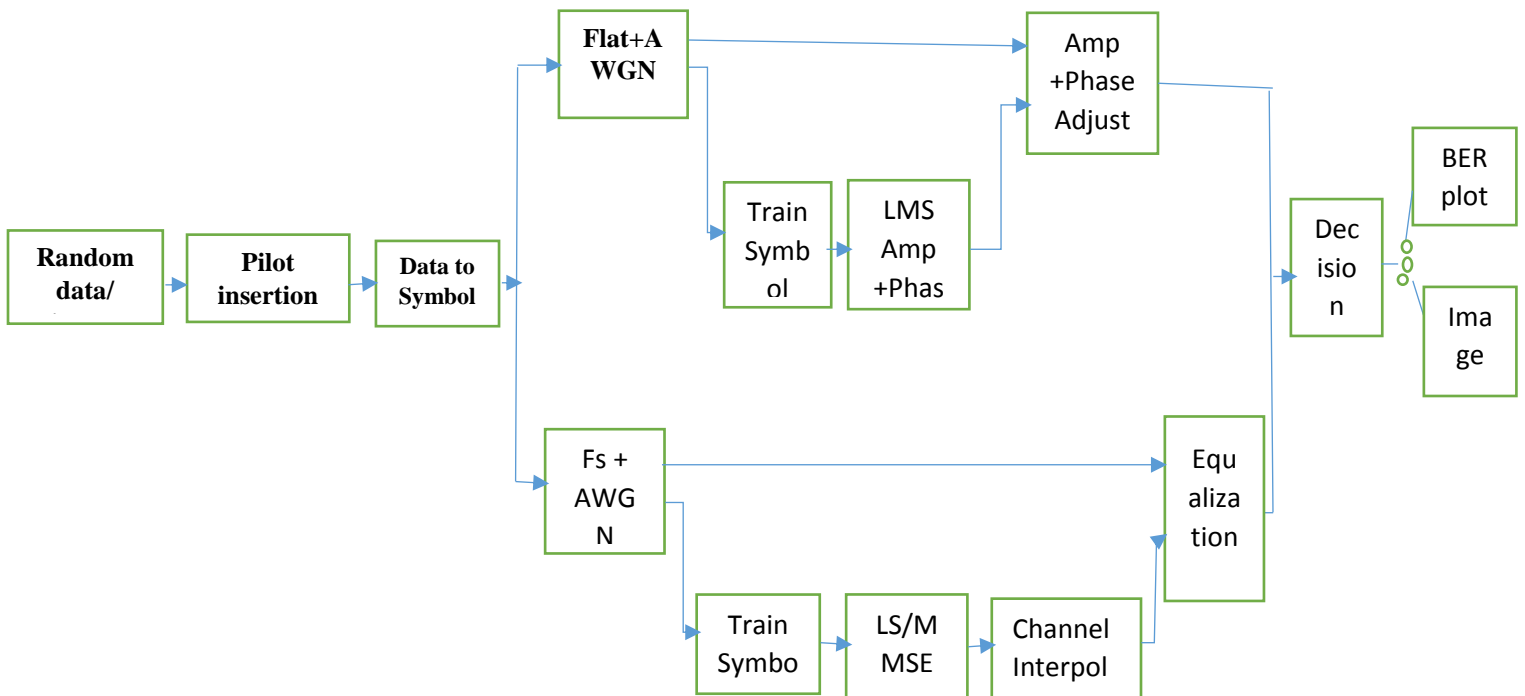


Figure 4.1: Channel estimation simulation diagram

The transmitter simulation diagram includes source encoder, train symbol generator and modulator, the input is encoded before train symbol insertion and modulation. Each complex data-valued complex symbol is allocated to a data subcarrier location. Complex symbols train symbols are generated and inserted at the kept train symbol subcarrier location for channel estimation and channel interpolation tenacity. In this thesis block type train symbol procedure is used and tested in $\frac{1}{4}$, $\frac{1}{8}$ and $\frac{1}{16}$ the data of train symbol ratio.

Source: - Two data types are used for the MATLAB result namely a randomly generate bits and an image files. Before encoding and modulation the image file is converted to data using image to data converter MATLAB function. The channel:-The medium from transmitter to receiver is expressed as multipath fading unknown channel. In this thesis we consider frequency selective and flat fading channels further corrupted by an AWGN. Channel estimation: in frequency selective channel using LS and MMSE algorithms channel is estimated. Channel interpolation:-after channel estimation the channel factors are interpolated at the data using interpolation techniques.

Table 4.1: Channel model parameters

Parameters	Value used
Modulation/Demodulation	QAM, 16QAM, 64QAM
Number of carriers	256
SNR	24dB
Channel model	PI,PO,RA6, TU6,Rayleigh
Channel BW	8MHZ

4.2. Results and Analysis

The MATLAB results for different channel models and modulation using the above listed parameters are given in the following section in the form of figures. The main purpose of channel model is to extract the channel factor and knowing the performance and to use wireless network communication systems.

4.2.1. Performance comparison of different channel models

Performance Comparison of Different Channel Models for QAM, 16QAM, 64QAM constellation

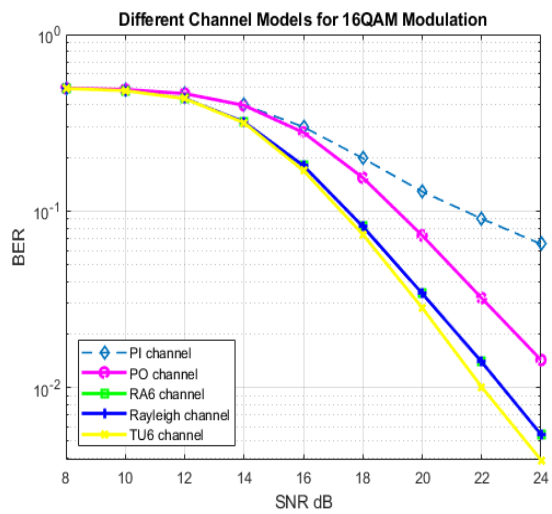
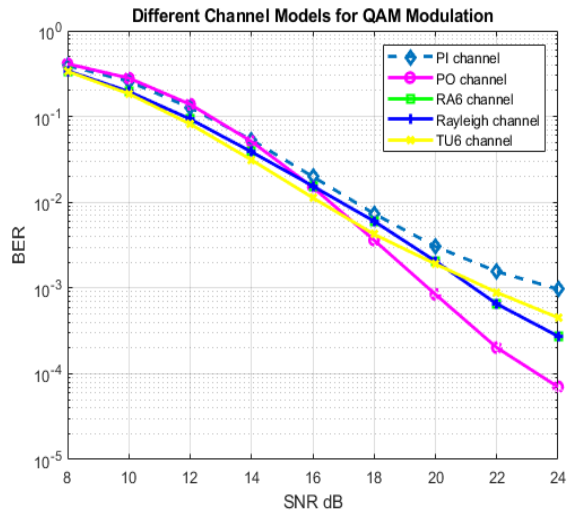


Figure 4.2: Different Channel Model for QAM Figure 4.3: Different channel model for 16QAM

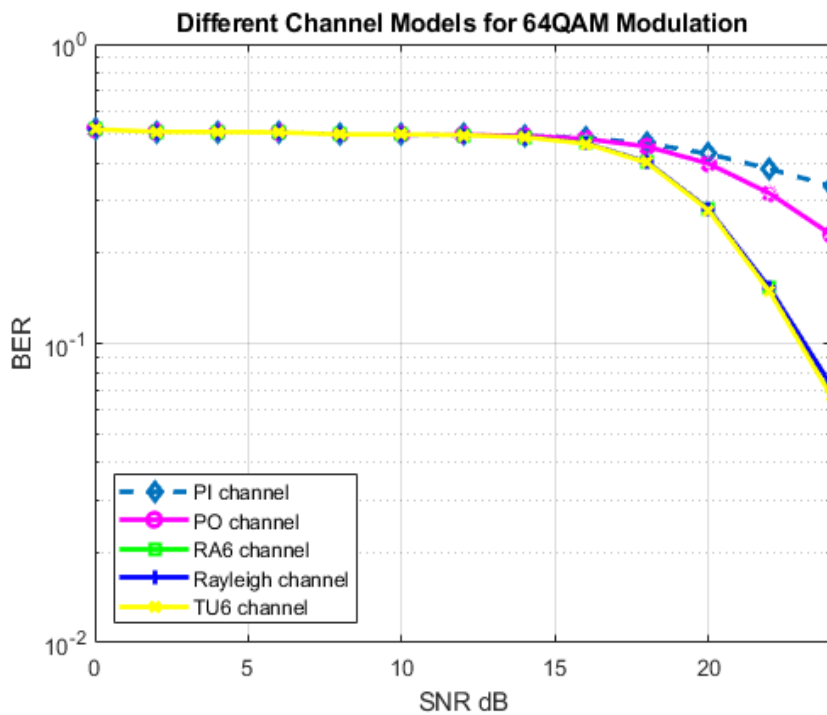


Figure 4.4: Different Channel model for 64QAM

From shown figure 4.2, 4.3, 4.4 that different channel models for different modulation order for QAM, 16QAM, 64QAM respectively. PI channel model which is the worst performance between all 5 channels at QAM constellation points. PO channel model is good performance at SNR of greater than 14dB for QAM constellation. The difference between PI and PO channel model are the length of the impulse response and the delay of output path. Channel models TU6 and RA6 are almost the same performance at all SNR levels for QAM. Similar to the system with QAM, we have almost the same performance both in Rayleigh and RA6 channels. It could be concluded that improvement obtained from having even one direct path to the receiver is much more effective than the distortions caused by the Doppler shift. The channel model system with 64QAM in the absence of direct path, using fixed receiver in TU6 channel is made the performance best among channels but still worst performance at this SNR value. We conclude that increase the SNR value to overcome the performance for TU6 channel model. Depending on channel characteristics, results in each channel have a different speed in their improvement this can be seen in difference of slopes. Smoother improvements in QAM, 16QAM, and 64QAM for different channel models.

4.2.2. Channel estimation parameter for LS and MMSE

The parameters used for channel model MATLAB are summarized in Table 4.4 below. The OFDM standard are presented in Chapter two. Besides the requirement of OFDM standard before extraction of the channel factor. From the different performance comparison the optimum values are selected for the implementation of channel model as listed in the table below.

Table 4.2: channel estimation parameters

Parameters	Value used
Modulation/Demodulation	QPSK
Modulation order	4
Input Format	TS
Estimation algorithm	LS and MMSE
Number of carriers	256
Pilot ratio	$\frac{1}{8}$ of the data
Pilot arrangement	Block type
SNR	15dB
Channel model	TU6
Number of channel taps	6,16
Channel interpolation	cubic spline
Channel BW	8MHZ
LMS step size	0.01

4.5. SNR VS BER performance comparison of LS and MMSE

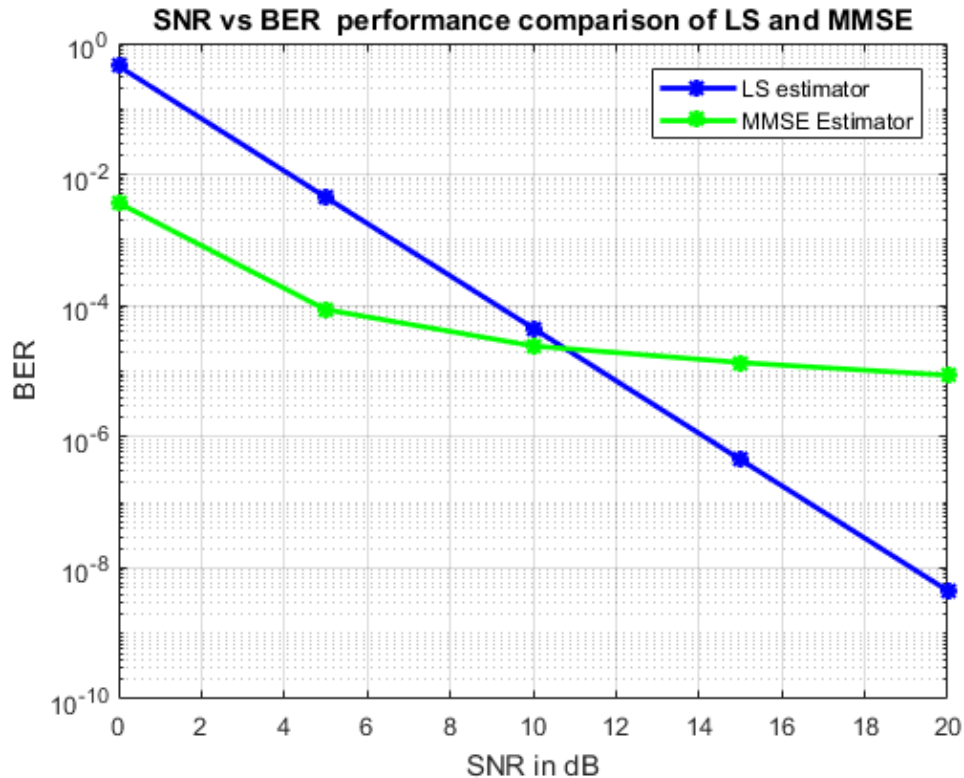


Figure 4.5: BER vs SNR plot of LS and MMSE channel estimators for QPSK modulation. From figure 4.3 show that the LS estimator is higher BER than MMSE estimators at low SNR value. the MMSE estimation techniques better than at LS estimator at lower SNR value up to SNR 11 dB and the result shown that at crossing point both value are equal so, we can both estimator at this point but after SNR 11dB LS estimator better BER value. The MMSE complexity is higher due to the channel correlation and the matrix inversion lemma.

4.5.2. Performance analysis of MMSE and LS channel estimation in different pilot size

SNR vs BER performance comparison of LS and MMSE in different pilot length

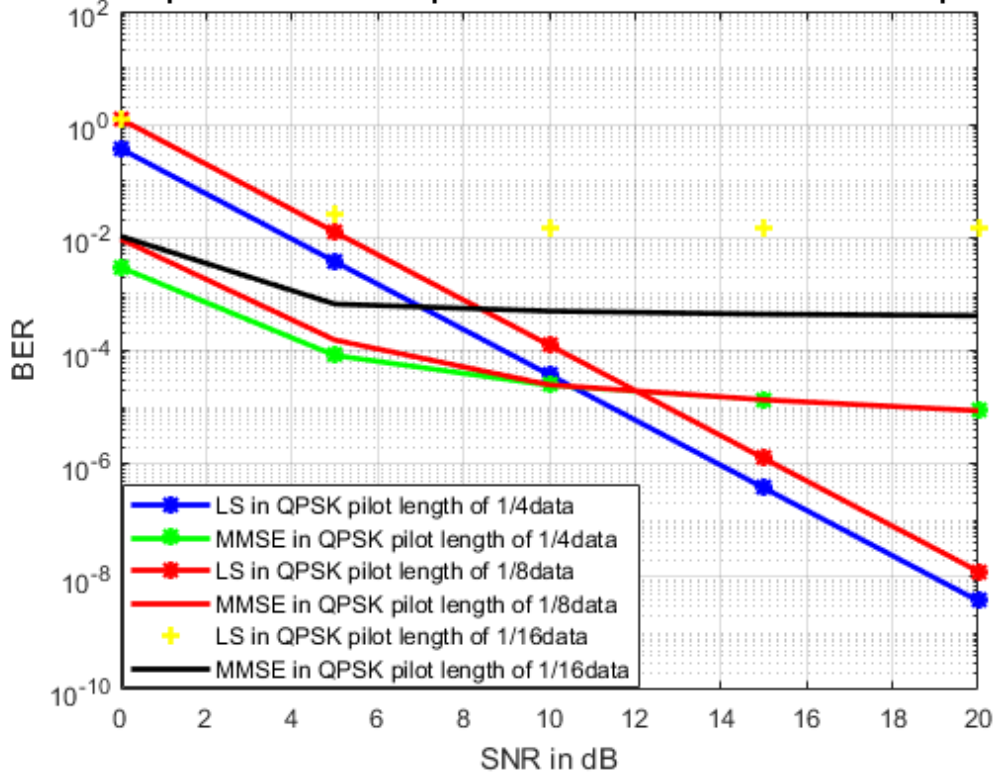


Figure 4.6: Performance comparison of LS and MMSE for different pilot sizes and CL

Table 4.3: Performance comparison of LS and MMSE

SN.	LS=1/4 CL=6	LS=1/8 CL=6	LS=1/16 CL=16	MMSE=1/4 CL=6	MMSE=1/8 CL=6	MMSE=1/ 16 CL=16
0	6.1×10^{-1}	9.95×10^{-1}	1.00	6×10^{-3}	1×10^{-2}	1×10^{-2}
4	1×10^{-2}	5.5×10^{-2}	6.05×10^{-2}	2.25×10^{-4}	5×10^{-4}	1×10^{-3}
8	4×10^{-4}	1×10^{-3}	1.15×10^{-2}	6×10^{-5}	7.15×10^{-5}	8.5×10^{-4}
12	7.5×10^{-6}	3×10^{-5}	1.05×10^{-2}	2.25×10^{-5}	2.25×10^{-5}	7.5×10^{-4}
16	1.05×10^{-7}	7.5×10^{-7}	1.05×10^{-2}	1.5×10^{-5}	1.5×10^{-5}	7.5×10^{-4}
20	6.05×10^{-9}	1.05×10^{-8}	1.05×10^{-2}	1×10^{-5}	1×10^{-5}	7.5×10^{-4}

There is always trade-off between the bandwidth efficiency and channel estimation accuracy regards the number of pilot symbols. The estimation becomes better when pilot size increases at the expense of bandwidth. As we can see from Figure 4.4 above using

MMSE algorithm we can achieve at lower SNR value the MMSE better performance but for higher SNR value and channel length lower LS channel estimation better performance and also channel length increase LS estimator poor BER value. Estimator becomes worst.in this thesis work for extract the channel coefficients 1/8 of the data pilot is used.

Table 4.4: channel estimation parameters

Parameters	Value used
Modulation/Demodulation	QPSK
Modulation order	4
Input Format	TS
Estimation algorithm	LS and MMSE
IFFT/FFT size	1k
Number of carriers	256
Pilot ratio	$\frac{1}{8}$ of the data
Pilot arrangement	Block type
SNR	15dB
Channel model	TU6
Number of channel taps	6
Cyclic prefix length	4
Channel interpolation	cubic spline
Channel BW	8MHZ
Sampling Fre.	10000Hz
LMS step size	0.01
Source image size	450 x450 pixels

4.6. Transmitted Original Image

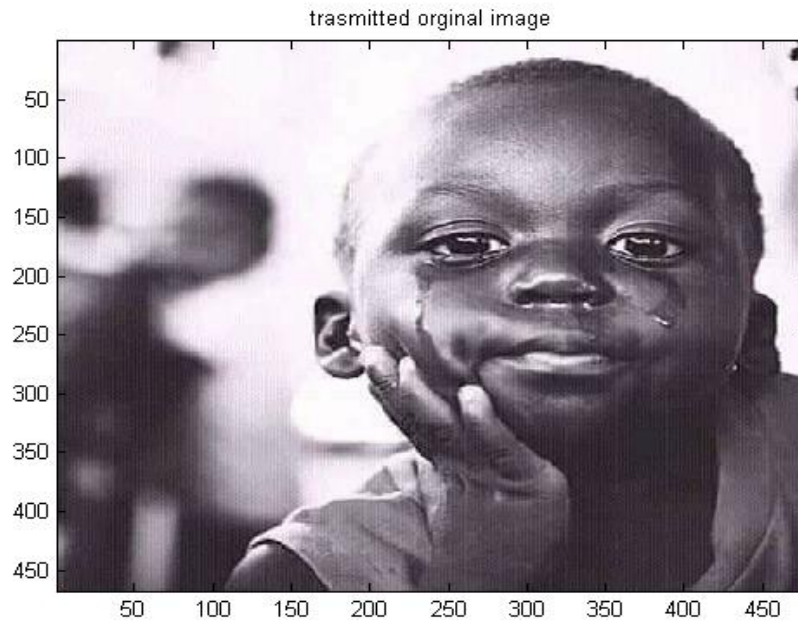


Figure 4.7: transmitted original image

In this work, two types of data are used to test the randomly generate bits and an image files. Obtained from the simulation experiment. The comparison results, obtained by using AWGN channel plus, flat and frequency selective channel are also included together with the main target which is frequency selective channel. To transmit and testing the image file of Figure 4.7 by considering the above table 4.4 parameter values and the image size taken to be 450×450 file is converted to digital data so, after gray coding and QPSK modulation the resulting signal is passed through AWGN and Frequency selective fading channels which results in the following results.

4.7. Constellation Plot in Flat Fading channel

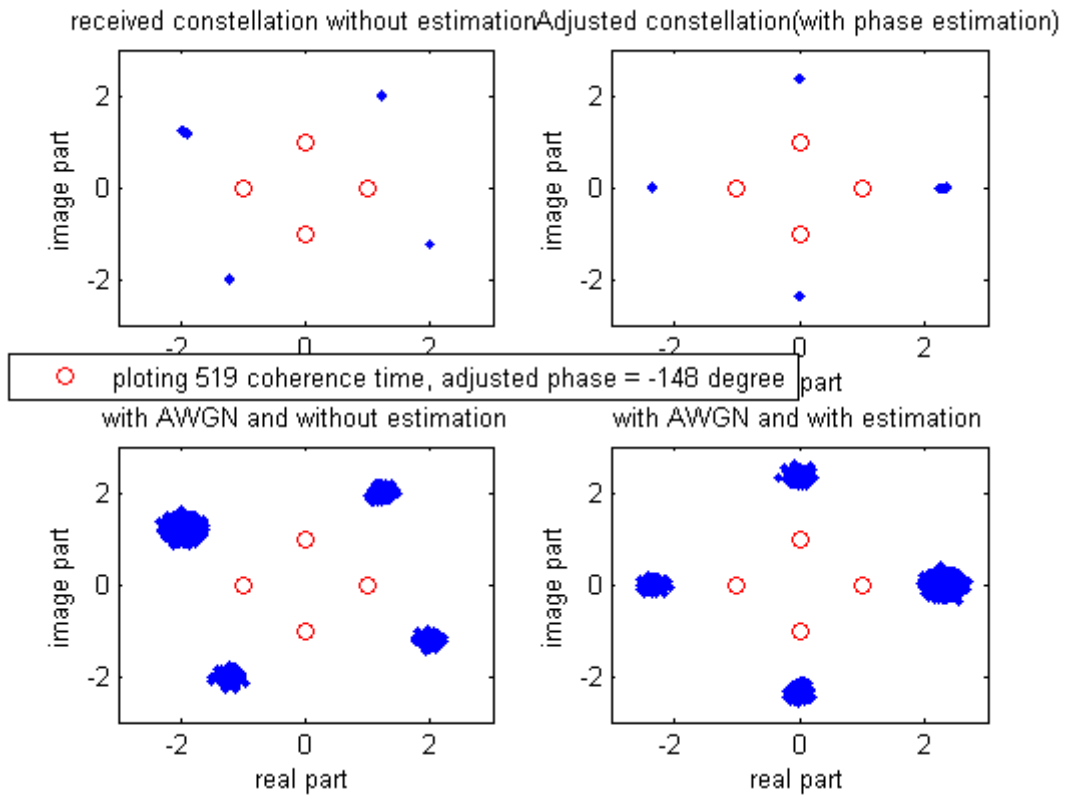


Figure 4.8: received and estimated constellation plot

In flat fading channel since there is no ISI the phase shifted can be adjusted using channel estimation. The Figure 4.8 above shows the received constellation is adjusted by 148 degree using channel estimator.

4.8. Constellation plot in frequency selective fading channel

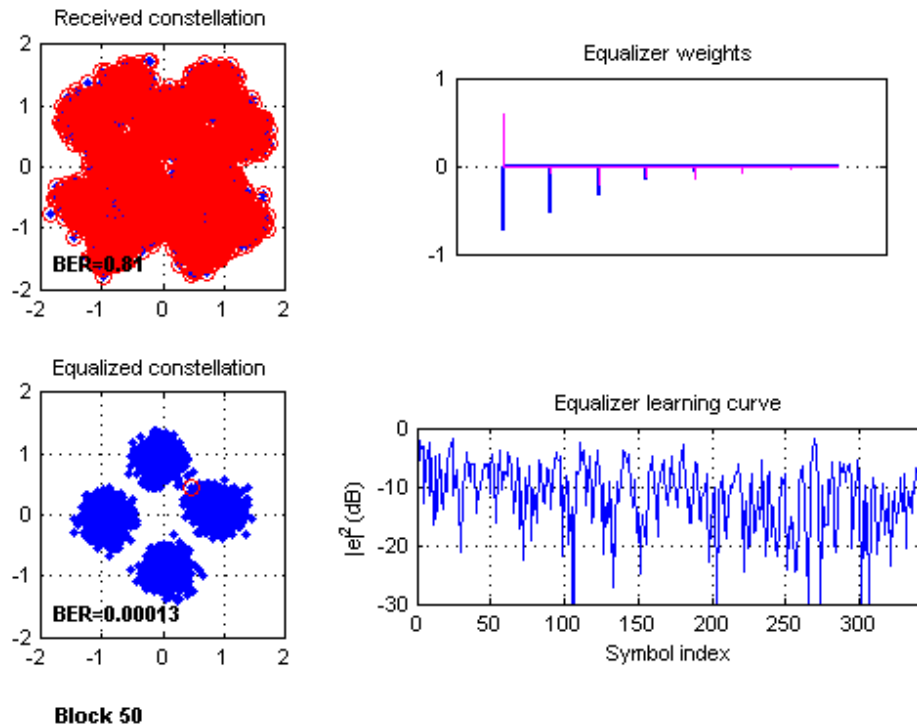


Figure 4.9: Constellation plot of MMSE equalizer at 15 dB SNR

Figure 4.9 show that, Red Cross are used to represent wrongly received bits while blue one is used to represent correctly received bits. From the first figure it is shown that the BER performance before equalization are 0.81 which means out of the transmitted 100 bits 81% is received wrongly. The second constellation plot shows the equalized constellation plot after passing the received constellation through MMSE equalizer. The training method used. In this plot the equalizer weights are complex valued numbers in which blue lines are used to represent their real values while magenta colored lines are used to represent the imaginary values of each equalizer weights. Here it is shown that the original QPSK constellation are recovered successfully after passing the QPSK demodulated signal through MMSE equalizer. Its BER performance is shown to be 0.00013 so, MMSE is does not support for high quality frame image transmission for wireless network communication systems at SNR 15dB for this work. To reduce BER increase the SNR value more than 15dB to overcome the performance of MMSE algorithm.

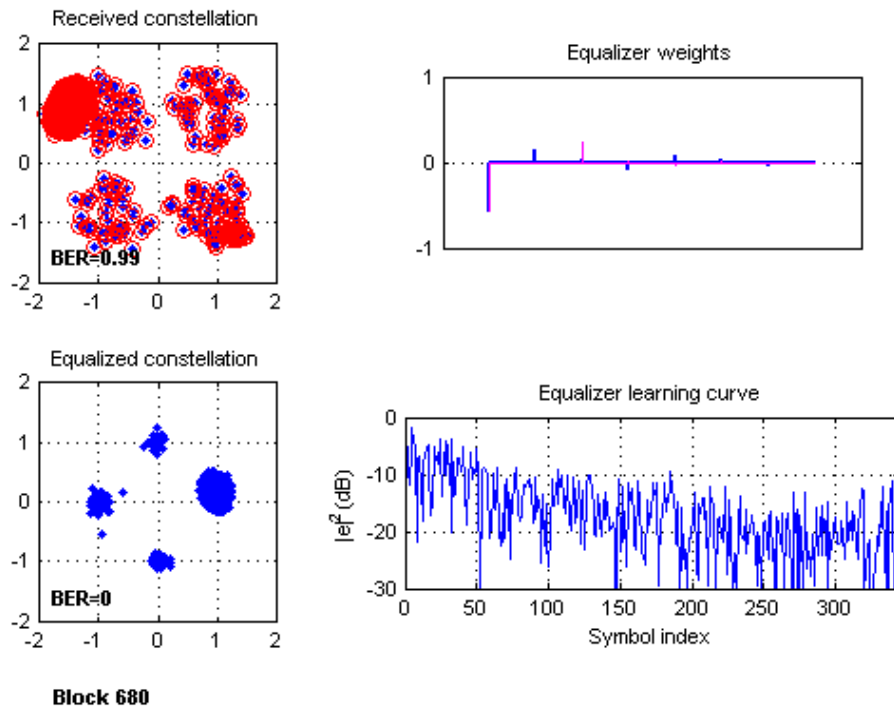
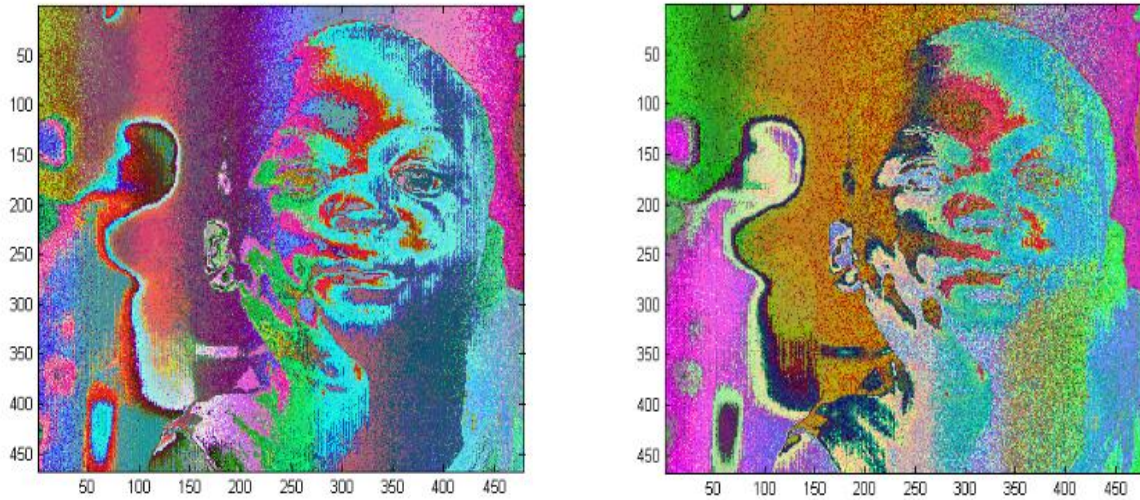


Figure 4.10: Constellation plot of MMSE equalizer at 15 dB SNR

Figure 4.10 it is shown that the BER performance before equalization are 0.99 which means out of the transmitted 100 bits 99% is received wrongly. The second constellation plot shows the equalized constellation plot after passing the received constellation through LS equalizer. In this plot the equalizer weights are complex valued numbers in which blue lines are used to represent their real values while magenta colored lines are used to represent the imaginary values of each equalizer weights. Here it is shown that the original QPSK constellation are recovered successfully after passing the QPSK demodulated signal through LS equalizer. Its BER performance is shown to be zero percent to reduce which are better for frame image transmission for high quality video transmission for terrestrial wireless network communication systems.

4.8.1. Received image comparison for MMSE and LS Channel estimation Algorithm



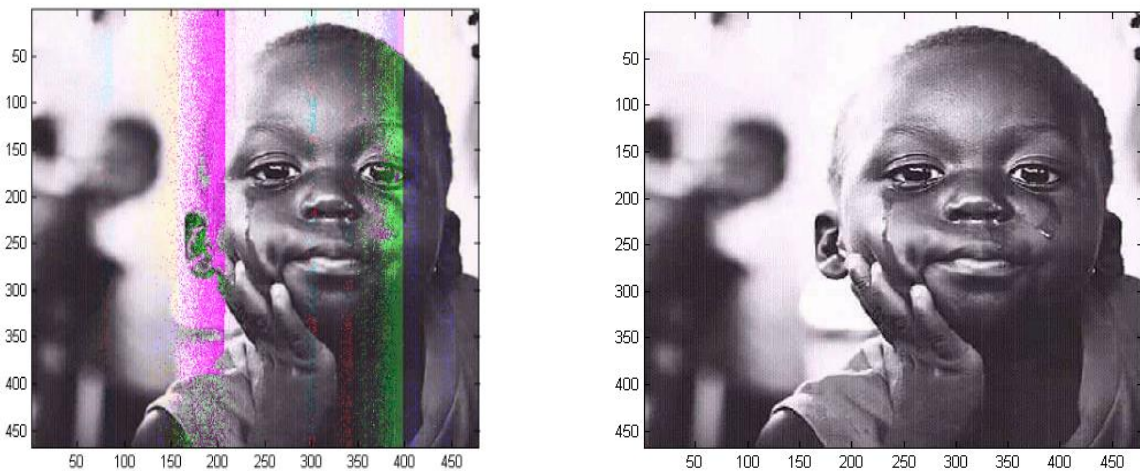
A) Received Image for MMSE

B) Received image for LS

Figure 4.11: Received image comparison for MMSE and LS 15 dB

Figure A and B shows the images received MMSE and LS estimation respectively considering the above table 4.4 parameter value. The received image are very erroneous and difficult to identify

4.8.2. Equalized image comparison for MMSE and LS Channel estimation Algorithm



A) Equalized Image for MMSE

B) Equalized image for LS

Figure 4.12: Equalized image for MMSE and LS at 15dB

Figure 4.12 A and B shows that equalized image for MMSE and LS after equalization respectively. Considering the above table 4.4 parameter value. The equalized image for LS is almost the same as the original transmitted image but MMSE does not show better improvement but as the signal power increases a better performance improvement is achieved.

Chapter Five: Conclusion and Future Work

5.1. Conclusion

In this thesis, a review of pilot-based channel estimation techniques for wireless network communication systems are given. Firstly, the general structure of channel estimation technique is taken by inserting the train symbol at the OFDM subcarriers and also channel estimation algorithms are revised. The MATLAB plot perform for QAM, 16QAM, and 64QAM constellations for different ITU channel models such as in PI, PO, RA6 six path, Rayleigh and TU6 six path channel models. Transmission and response result is shown that by increasing the number of constellation point, BER performance gets worse. It is caused by loss of orthogonality of the OFDM subcarriers. Due to the fast varying multipath path fading channel conditions at high data rates.

The performance of LS and MMSE are compared based on their channel length and pilot ratio performance of LS and the MMSE estimators and computational complexity are compared. Based on the performance analysis the MMSE estimator has better than LS estimator at the low SNR value. MMSE estimator aches from high computational complexity due to this factor at the expense of bandwidth low performance at higher SNR compared to LS estimator. The use of a channel estimation techniques appears to play a significant role in clearing the raster in the received picture by removing the noise and ISI in the received signal. From the simulation results, the LS equalizer in frequency selective channel needs to recover corrupted image signal successfully. Which is the BER performance is found to better performance at 15dB SNR, this BER performance is sufficient for high quality frame image transmission for wireless terrestrial network communication systems in TU6 path channel model.in the other hand MMSE channel estimator is not good enough at 15dB for frame image transmission so, to overcome MMSE estimator is increase SNR value more 15dB for this work.

5.2. Future Work

There are a few open areas for future works for wireless network communication for OFDM systems, in this thesis the analysis is on train symbol-based channel estimation techniques, which is bandwidth inefficient. Semi-blind channel estimation techniques can improve the band width efficiency since it requires less train symbol length than non-blind techniques and have better performance than totally blind channel estimation techniques. Therefore, performance of semi-

blind channel estimator could be one area of future study. In this analysis, all channels is assumed to be slow-fading. In a case of fast fading channels and channel fading coefficients vary within a symbol assumption does not hold. Therefore, performance of channel estimator in fast fading channel environments could be one area of future study. In this thesis all the train symbols are assumed as orthogonally arranged which is appropriate for one dimensional channel estimators i.e. frequency selectivity taken in this thesis time selectivity not considered. But two dimensional (doubly selective) estimations techniques that can be implemented using basis expansion model (BEM) and are more efficient one of the feature work.

REFERENCE

- [1] I. Eizmendi, M. Velez, D.G. Barquero, Morgade, V. B. Lecuyer, M.Slimani, and J. Zoellner, “*The Second Generation of Terrestrial Digital Video Broadcasting System*”, IEEE Transactions on Broadcasting, Vol.60, NO.2, pp.258-271, 2014.
- [2] W. Liping, “*Channel Estimation and Combining Orthogonal Pilot Design in MIMO-OFDM System*”, urnal of Networks, Vol. 9, No. 2, February 2014.
- [3] A. Rana, M. Arora, “*Channel Estimation by using Pseudo-Pilot in OFDM systems*”, International Journal of Engineering Trends and Technology (IJETT) Volume-45 Number7 March 2017.
- [4] V. Mathai, K. M. Sagayam, “*Comparison and Analysis of Channel Estimation Algorithms in OFDM Systems*” International Journal of Scientific & Technology Research Volume 2, Issue 3, March 2013.
- [5] I. P. Astawa, T. B. Santoso, P. Elektronika and N. Surabaya, “*Analysis of Performance DVB- T2 Using MIMO System Over MMSE Channel Estimation*”, IEEE Region 10 Symposium (TENSYMP), Bali, Indonesia 2018.
- [6] H. Vasava, “*Performance Analysis of Channel Estimation using Pilot Technique,*” IJSRD - International Journal for Scientific Research & Development| Vol. 4, Issue 12, 2017.
- [7] A. K. Shrives, “*Comparative Analysis of LS and MMSE Channel Estimation Techniques for MIMO-OFDM System*” IJIRST –International Journal for Innovative Research in Science & Technology| Volume 1Issue 8 |January 2017.
- [8] R. A. Varma, M. S. Krishna, “*Estimation of Channel in OFDM Wireless Channel using Ls And MMSE techniques*”, International Journal of Electronics and Communication Engineering and Technology (IJECET) Volume7, Issue 3, may–June 2016.
- [9] A. Gupta, A. Potnis,” *CS Based Channel Estimation for OFDM Systems under Long Delay Channels Using MATLAB*”, Abhishek Gupta. Int. Journal of Engineering Research and Application”, ISSN: 2248-9622, Vol. 6, Issue 12, Part -3 December 2016, pp.74-78

- [10] G. M. Hassan, K. A. Abu Baker, and M. R. Mokhtar, “*Sending Image in Noise Channel using Orthogonal Frequency Division Multiplexing Scheme*”, Journal of Theoretical and Applied Information Technology 30th June 2018. Vol.96. No 12
- [11] M. A. Mohammed, M. Wangdong and A. Z. Ali, “*MIMO Channel Estimation Using the LS and MMSE Algorithm*”, IOSR Journal of Electronics and Communication Engineering (IOSR-JECE) e-ISSN: 2278-2834, p- ISSN: 2278- 8735. Volume12, Issue 1, Ver. II (Jan.-Feb. 2017), PP 13-22.
- [12] H. Banaba, P. Mary, J. François Heard, Youssef Nasser, and Oussama Baozi, ‘*Spectral Overlap Optimization for DVB-T2 and LTE Coexistence*’, IEEE Transactions on broadcasting this article has been accepted for inclusion in a future issue of this journal. Content is final as presented, with the exception of pagination 2018 IEEE.
- [13] S. Zettas, P. I. Lazaridis, Z. D. Zaharis, S. Kasampalis and J. Cosmas, “*Performance Comparison of LS, LMMSE and Adaptive Averaging Channel Estimation (AAE) for DVB-T2*”, IEEE BMSB 2015 Conference.
- [14] T. Rappaport, “*Wireless communication*”: Principle and Practice, 2nd ed., Singapore: Pearson Education, 2002.
- [15] L. Dai, B. Wang, Y. Yuan, S. Han, C. I. I and Z. Wang, “*Non-orthogonal multiple access for 5G: solutions, challenges, opportunities, and future research trends*,” IEEE Commun. Mag., vol. 53, no. 9, pp. 74-81, Sep. 2015.
- [16] M. Morshed, “*Synchronization performance in DVB-T2 system*,” MSC thesis, Tamere, 2009
- [17] Y. X. Jian Wang, “*Behavior Modeling of a Digital Video Broadcasting System and the Evaluation of its Equalization Methods*,” Linköping, 18th March 2017.
- [18] COST207, “*Digital land mobile radio communications (final report)*,” commission of European communities, 1989.

- [19] M. Sohail and T.Y.Al-Naffouri, "An em based frequency domain channel estimation algorithm for multi access OFD systems," Elsevier Journal of Signal Processing, vol. 10, pp. 1562–1572, 2010.
- [20] P. Venkateswarlu. "Channel Estimation techniques in MIMO OFDM LTE systems" Int. Journal of Engineering Research and Applications ISSN: 2248-9622, Vol. 4, Issue 7(version1) July 2014, and pp. 157-161
- [21] D. Jaeger, C. Schaaf," *High Performance Data Transmission on Cable Technology, Implementation, Networks*", Shaker Verlag Aachen 2010.
- [22] J. Morgade, P. A. Frank, "SFN-SISO and SFN-MISO gain performance Analysis for DVB-T2 Network Planning," IEEE Transactions on Broadcasting, June 2014.
- [23] J. T. C. (. B. o. t. European, "Digital Video Broadcasting (DVB; Implementation guidelines for a second generation digital terrestrial television broadcasting system (DVB-T2)," European Broadcasting Union, Geneva, June 2016.
- [24] Progira parts of s-group, "Why the Choice of T2-Frame Length is Essential for DVB-T2" Network coverage Infrastructure Investment Optimization, Nov 11, 2013. [Online].Available: <https://www.progira.com/news/choice-t2-frame-length-essential-dvb-t2>. [Accessed: Nov.3, 2018]
- [25] M. S. Morshed, "Synchronization Performance in DVB-T2 System". Tampere University of Technology Faculty of Computing and Electrical Engineering on 04.03.2009.
- [26] N. Cornillet, M. Crussi`ere, J. Fran, C.´ elard, "Performance of the DVB- T2 System in a Single Frequency Network: Analysis of the Distributed Alamouti Scheme," in IEEE International Symposium, Nuremb erg, Germany, Jun 2011.
- [27] V. Von, J. Metzger, "Variance of DVB-T2 Performance Gains over different channels," 2009.
- [28] J. Vlaović, S. R. Drlje and G. Horvat, "Overview of OFDM Channel Estimation Techniques for DVB-T2 Systems," Universit at des Saarlandes Naturwissen schaftlich-Technische Fakultat Fachrichtung Computer-und Kommuni kationstechnik IEEE, 2016.

- [29] M. X. Chang, Member, IEEE, ‘*Analytic Comparison for Channel Response Estimation Based on Time- and Frequency-Domain Pilot Signals,*’ IEEE Transactions On Vehicular Technology, Vol. 64, No. 9, September 2017.
- [30] S. Lambotharan, J. Chambers and J. Johnson C. R.,”*Attraction of saddles and slow Convergence in CMA adaptation*”, Signal processing 59 (1997), pp. 335-340.
- [31] Q. Sun, S. Han, I. C. Lin, and Z. Pan, “On the ergodic *Capacity of MIMO NOMA systems,*” IEEE Wireless Commun. Lett. vol.4, no.4, pp. 405-408, Aug. 2015.
- [32] L. Li, H. Fan, “*Blind CDMA detection and equalization using linearly Constrained CMA*”, In Proc. Int. Conf. Acoustics, speech and signal processing (Istanbul, Turkey, 2000), vol. 5. Pp. 2905-2908.
- [33] J. K .Tugnait, T. Li, “*Blind asynchronous multiuser CDMA receivers for ISI Channels using code-aided CMA*”, IEEE J. Select. Areas Commun. 19 (2001), pp. 1520-1530.
- [34] K. Kumar, A. Grover, “*Comparison of Block Type Pilot Channel Estimation Techniques for evaluating the performance of OFDM,*” International Journal of Scientific & Engineering Research, Volume 3, Issue 11, November-2012 1ISSN 2229-5518
- [35] L. M. Jiménez, "*Channel Estimation Architectures For Mobile Reception In Emerging DVB Standards,*" May 2012.
- [36] M. Mendicute, I. Sobrón, L. Martínez and P. Ochandiano, "*DVB-T2: New Signal Processing Algorithms for a Challenging Digital Video Broadcasting Standard, Digital Video,*" InTech, China, February, 2010.
- [37] Y. Zhang, F. Salman and J. Cosmas, "*Modelling and Performance of a DVB-T2 Channel Estimator and Equaliser for Different Pilot Patterns,*" IEEE.
- [38] A. Rizaner, Shahrzad Kavianirad, and H. Amca,” *Channel Estimation and Equalization of DVB-T in Fast Fading Multipath Channels*”, Lecture Notes on Information Theory Vol. 3, No. 2, December 2015.

- [39] ETSI, "*Digital Video Broadcasting (DVB); Frame structure channel coding and modulation for a second generation digital terrestrial television broadcasting system (DVB-T2) ETSI EN 302 755*," Tech. rep., 2009.
- [40] E. T. 102, "*Digital Video Broadcasting (DVB); Implementation guidelines for a second generation digital terrestrial television broadcasting system (DVB-T2)*," V1.2.1, 2012.
- [41] Dr. Sheng-Chou Lin, "Small-scale Multipath Propagation", *Wireless Communication*, [Online]:<https://www.google.com/search?ei=9mCqXPfwG87QkwWxoY=small+scale+multipath+propagation>, [Accessed: Nov.7, 2018]
- [42] L. Polak T. Kratochvil, "*Simulation and Measurement of the Transmission Distortions of the Digital Television DVB-T/H Part 3: Transmission in Fading Channels*", *Radio engineering*, vol. 19, pp. 703-711 2016.
- [43] European Telecommunications Standards Institute, "*Digital Video Broadcasting (DVB): Measurement guidelines for DVB systems*" European Telecommunications Standards Institute, ETSI TR 101 290 V1.2.1 2001.
- [44] European Telecommunications Standards Institute (2006) "*Digital Video Broadcasting (DVB): Second generation framing structure, channel coding and modulation systems for Broadcasting, Interactive Services, News Gathering and other broadband satellite applications*" European Telecommunications Standards Institute, ETSI EN 302 307 V1.1.2.
- [45] B. Eriz, G. Eizmendi., "*Laboratory Tests for testing DVB-T2 mobile performance*," Conference: Broadband Multimedia Systems and Broadcasting (BMSB), 2011 IEEE International Symposium on
- [46] P. Ing, T. Kratochvíl, "*Analysis of Transmission Distortions in Digital Television DVB-T/H*," 2009.
- [47] European Telecommunications Standards Institute, "*Digital Video Broadcasting (DVB): Implementation guide for DVB terrestrial services; transmission aspects*," European Telecommunications Standards Institute, ETSI-TR-101, 2007. [Online].Available: <http://www.etsi.org>. [Accessed: Des. 5, 2018].

- [48] T. Kratochvil, "DVB-T/H Portable and Mobile TV Performance", Purkyňova 118, 61200 Brno, Czech Republic, LNICST 16, pp. 163–174, 2009.
- [49] M. Mendicute, I. Sobrón, L. Martínez and P. Ochandiano, "DVB-T2: New Signal Processing Algorithms for a Challenging Digital Video Broadcasting Standard, *Digital Video*," InTech, China, February, 2010.
- [50] M. Dąbrowski, "Investigation of Digital Terrestrial Television Receiver Architectures for DVB-T2 Standard," Ph. D. Thesis, Warsaw, 2017.
- [51] S. Kavianirad, "Performance of DVB-T System under Multipath Fading with LS Channel Estimation and Equalization", Eastern Mediterranean University August 2015
- [52] ETSI, "Digital Video Broadcasting (DVB); Frame structure channel coding and modulation for a second generation digital terrestrial television broadcasting system (DVB-T2) ETSI EN 302 755," Tech. rep., 2009.
- [53] M. Morshed, "Synchronization performance in DVB-T2 system," Tampere University of Technology, September 2015.
- [54] L. M. Jiménez, "Channel Estimation Architectures For Mobile Reception In Emerging DVB Standards," May 2017.
- [55] E. T. 102, "Digital Video Broadcasting (DVB); Implementation guidelines for a second generation digital terrestrial television broadcasting system (DVB-T2)," V1.2.1, 2017. [Online]. Available: <https://www.progira.com/news/choice-t2-frame-length-essential-dvb-t2>. [Accessed: June.3, 2018]
- [56] A. B. Singh¹, V. K. Gupta, "Performance Evaluation of MMSE and LS Channel Estimation in OFDM System", International Journal of Engineering Trends and Technology (IJETT) – Volume 15 Number 1 – Sep 2014
- [57] J. Morgade, P. Angueira and J. Frank, "SFN-SISO and SFN-MISO gain performance Analysis for DVB-T2 Network Planning," IEEE Transactions on Broadcasting, June 2014.

- [58] J. Hwang, “*Simplified Channel Estimation Techniques for OFDM Systems with Realistic Indoor Fading Channels*”, Waterloo, Ontario, Canada, 2009 c Jake Hwang, 2009
- [59] C. R. N. Athaudage and A. D. S. Jayalath, “*Enhanced MMSE channel estimation using Timing error statistics for wireless OFDM systems*”. IEEE Trans. Broadcast., 50(4), Dec. 2004.
- [60] S. Y. Cho, J. Kim, W.Y. Yang and C. G. Kang, “*MIMO-OFDM Wireless Communications With MATLAB*”, Singapore: John Wiley & Sons (Asia) Pte Ltd, 2010.
- [61] Y. Zhang, F. Salman and J. Cosmas, “*Modelling and Performance of DVB-T2 Channel Estimator and Equaliser for Different Pilot Patterns*,” IEEE.
- [62] K. Eneman. ECEg-6021.Class Lecture, ‘*Topic: “Adaptive filters*”, School of Electrical and Computer Engineering, HGPP Project, Hawassa Institute Of Technology, Ku Leuven, April 2017
- [63] M. Hsieh, C. Wei. “*Channel estimation for OFDM systems based on comb-type pilot arrangement in frequency selective fading channels.*” IEEE Trans. Consumer Electron, 44(1), 217–228, 1998.
- [64] S. K. Bandari, V. M. Vakamulla, and A. Drosopoulos,” *Training Based Channel Estimation for Multi taper GFDM System*”, 1Electronics & Communication Engineering, National Institute of Technology, Warangal 506004, India, Volume 2017, Article ID 4747256, 8 pages, 1 October 2017
- [65] K. Hariprasad, S. Sandeep, “*An Interpolation Technique for Channel Estimation in OFDM*” Systems, Manikanta C. International Journal of Science and Research (IJSR) ISSN (Online): 2319-7064 Index Copernicus Value (2013): 6.14/ Impact Factor (2013) 4.438.
- [66] P. Yuvapoositanon, “*Blind Adaptive Techniques for Direct-sequence Code Division Multiple Access Receivers*”, Ph.D. dissertation, university of London, 2015.

- [67] C. Shin, R. W. Heath, and E. J. Powers, “*Blind channel estimation for MIMO-OFDM systems*,” IEEE Trans. Veh. Tech., vol. 56, pp. 70–685, Mar. 2007.
- [68] V. Buchoux, O. Cappe, E. Moulines, and A. Gorokhov, “*On the performance of semi-blind subspace-based channel estimation*,” IEEE Trans. Signal Proc., vol. 48, pp. 1750–1759, June 2000.